MCB
Journals.ASM.org

GATA-6 and NF-κB Activate CPI-17 Gene Transcription and Regulate Ca^{2+} Sensitization of Smooth Muscle Contraction

Ettickan Boopathi,[a] Joseph A. Hypolite,[a] Stephen A. Zderic,[b] Cristiano Mendes Gomes,[c] Bruce Malkowicz,[a] Hsiou-Chi Liou,[d] Alan J. Wein,[a] Samuel Chacko[a,e]

Division of Urology, University of Pennsylvania, Glenolden, Pennsylvania, USA[a]; Department of Urology, Children's Hospital of Philadelphia, Philadelphia, Pennsylvania, USA[b]; Hospital das Clinicas, University of Sao Paulo School of Medicine, Sao Paulo, Brazil[c]; Division of Immunology, Department of Medicine, Weill Medical College of Cornell University, New York, New York, USA[d]; Department of Pathobiology, University of Pennsylvania, Philadelphia, Pennsylvania, USA[e]

Protein kinase C (PKC)-potentiated inhibitory protein of 17 kDa (CPI-17) inhibits myosin light chain phosphatase, altering the levels of myosin light chain phosphorylation and Ca^{2+} sensitivity in smooth muscle. In this study, we characterized the CPI-17 promoter and identified binding sites for GATA-6 and nuclear factor kappa B (NF-κB). GATA-6 and NF-κB upregulated CPI-17 expression in cultured human and mouse bladder smooth muscle (BSM) cells in an additive manner. CPI-17 expression was decreased upon GATA-6 silencing in cultured BSM cells and in BSM from NF-κB knockout (KO) mice. Moreover, force maintenance by BSM strips from KO mice was decreased compared with the force maintenance of BSM strips from wild-type mice. GATA-6 and NF-κB overexpression was associated with CPI-17 overexpression in BSM from men with benign prostatic hyperplasia (BPH)-induced bladder hypertrophy and in a mouse model of bladder outlet obstruction. Thus, aberrant expression of NF-κB and GATA-6 deregulates CPI-17 expression and the contractile function of smooth muscle. Our data provide insight into how GATA-6 and NF-κB mediate CPI-17 transcription, PKC-mediated signaling, and BSM remodeling associated with lower urinary tract symptoms in patients with BPH.

Phosphorylation of myosin light chain (MLC_{20}) by a Ca^{2+}/calmodulin-dependent myosin light chain kinase (MLCK) is implicated in the regulation of actomyosin ATPase and contraction in smooth muscle and nonmuscle cells (1). Myosin light chain phosphatase (MLCP) dephosphorylates MLC_{20}, resulting in relaxation of smooth muscle (1). Under certain physiological conditions, smooth muscles produce tone without the increase in cytosolic Ca^{2+} required to activate MLCK (2, 3). This increased Ca^{2+} sensitivity (Ca^{2+} sensitization) is achieved through a G protein-coupled signaling mechanism that decreases MLCP activity via phosphorylation of the myosin-targeting subunit (MYPT1) by RhoA-activated kinase (ROCK) (3–5). In addition, MLCP is regulated by a second signaling pathway mediated by CPI-17 (protein kinase C [PKC]-potentiated inhibitory protein of 17 kDa, also known as PPP1R14A), particularly in tonic smooth muscles (6). CPI-17 is primarily expressed in smooth muscle and neuronal tissues (7–9), and a biochemical circuit involving PKC-mediated activation of CPI-17 modulates the distinct physiological processes of vascular contractility and cerebellar long-term synaptic depression (7). CPI-17 is a phosphorylation-dependent inhibitor of myosin phosphatase, and phosphorylation of this protein at Thr^{38} by PKC in response to agonists increases its inhibitory potency toward MLCP (8). Thus, PKC and RhoA/ROCK-mediated pathways, acting through CPI-17 and MYPT1, respectively, play a major role in force generation and maintenance by inhibiting MLCP activity, resulting in an increase in myofilament Ca^{2+} sensitivity (2). This calcium sensitization is believed to play a role in maintaining the normal tone of smooth muscle (3, 4) and is important for retention of the resting tone of visceral organs, including the urinary bladder during the filling phase.

Deregulation of CPI-17 expression and phosphorylation has been linked to pathological conditions associated with smooth muscle contractile dysfunctions, such as intestinal bowel disease (10), asthma (11), pulmonary hypertension (12), vasoconstriction (13), diabetes (14, 15), obstruction-induced bladder smooth muscle (BSM) hypertrophy (16), and certain tumors (17). Therefore, CPI-17 is an important potential pharmaceutical target in the treatment of a myriad of diseases. In colonic smooth muscle, CPI-17 expression and phosphorylation are blocked by interleukin-1β (IL-1β), which inhibits both the initial and sustained contraction (18). Conversely, in aortic smooth muscle, CPI-17 transcription is increased by transforming growth factor beta (TGF-β), IL-1β, and tumor necrosis factor alpha (TNF-α) (19).

We sought to identify the transcription machinery critical for CPI-17 transcription and elucidate the mechanism of CPI-17 upregulation during BSM hypertrophy in partial bladder outlet obstruction (PBOO), induced surgically in mice and caused by benign prostatic hyperplasia (BPH) in men. Using a combination of protein purification by DNA affinity chromatography, mutational analysis, and chromatin immunoprecipitation, we demonstrate for the first time that in BSM, GATA-6 and nuclear factor kappa B (NF-κB) activate CPI-17 gene expression through their cognate binding sites in its promoter, and further, we show that NF-κB regulates PKC-mediated signaling in BSM contraction.

Received 14 May 2012 Returned for modification 23 June 2012
Accepted 23 December 2012
Published ahead of print 28 December 2012
Address correspondence to Samuel Chacko, chackosk@mail.med.upenn.edu.
Supplemental material for this article may be found at http://dx.doi.org/10.1128/MCB.00626-12.

doi:10.1128/MCB.00626-12

MATERIALS AND METHODS

Cloning, plasmid construct preparation of primary BSM cells, transient transfection, and promoter activity assays. A 1.333-kb 5′ upstream sequence of the CPI-17 (PPP1R14A) gene was amplified from mouse genomic DNA with gene-specific primers designed using the GenBank nucleotide sequence (accession number NM_026731). Amplified DNA fragments were subcloned into the pGL4 basic luciferase reporter vector (pGL4.1; Promega, Madison, WI). Truncations of the promoter were carried out by PCR using the 1.333-kb CPI-17 promoter as the template and subcloned into pGL4. Mutations within the CPI-17 promoter were created using a QuikChange site-directed mutagenesis kit according to the manufacturer's directions (Stratagene, La Jolla, CA). We performed site-directed mutagenesis at the κB core binding site in the 1.33-kb murine CPI-17 promoter, yielding the mutant Mut1, and at multiple GATA motifs (−1233 to −1263) in the CPI-17 promoter, yielding Mut2. The double mutation of both Mut1 and Mut2 was designated Mut3.

GATA-6, NF-κB p50, and c-Rel cDNA was obtained from OriGene Technologies, Inc. (Rockville, MD). Primary BSM cells were prepared from mouse bladders as described previously (20). Briefly, the bladder urothelial and serosal layers were removed from 8-week-old mice and the remaining muscle layer was dissected into small pieces. BSM cells were dissociated with collagenase (Sigma-Aldrich Co., St. Louis, MO), and the isolated cells were cultured in M199 supplemented with 10% fetal bovine serum, 1% vitamins, and 1% antibiotics-antimycotics. Cultured cells were identified as smooth muscle cells by the presence of smooth muscle-specific α-actin and myosin using immunofluorescence and immunoblot analyses, respectively. Human primary BSM cells were obtained from Lonza Walkersville, Inc. (Walkersville, MD). Plasmids were transfected into murine and human primary BSM cells by electroporation using Amaxa Nucleofector II (Lonza Walkersville, Inc.) according to the manufacturer's instructions. *Renilla* luciferase was included in all transfections for normalization of transfection efficiency. Firefly and *Renilla* luciferase activities were determined using a dual-luciferase reporter assay system (Promega, Madison, WI). Cleared extracts (100 μl per well) were prepared using the passive lysis buffer provided, and luciferase activity was measured according to the manufacturer's instructions.

Bioinformatics analyses. The TATA box in the murine CPI-17 promoter was predicted using the Matrix Family Library, version 8.4, of Genomatix MatInspector software (http://www.genomatix.de/online_help/help_matinspector/matinspector_help.html) (21). The CPI-17 promoter sequences of human, mouse, and rat were aligned using the bioinformatics tool ClustalW (http://www.genome.jp/tools/clustalw) (21).Various bioinformatics tools and programs, including Match-Public (www.gene-regulation.com/cgi-bin/pub/programs/match/match.cgi), AliBaba2 (http://www.gene-regulation.com/pub/programs/alibaba2/index.html), and Transcription Element Search software, which utilizes the Transcription Factor Database (http://www.cbil.upenn.edu/cgi-bin/tess/tess), were used to identify transcription factor binding sites on the CPI-17 promoter.

Surgical induction of PBOO in a mouse model. All procedures for creating PBOO mice were approved by the Institutional Animal Care and Use Committee at the Children's Hospital and the University of Pennsylvania. Adult male mice were subjected to partial surgical ligation of the urethra as previously described (22). Sham-operated animals underwent an identical procedure until the suture was tied down, at which point the suture was removed and the abdomen closed. After the desired time, the mice were anesthetized, the bladder harvested, and the BSM layer separated from the mucosa and serosa.

Human bladder samples. After obtaining institutional review board (IRB) approval (IRB 803645), we received frozen bladder tissue samples (collected through IRB protocol number 811/04) from the University of Sao Paolo, Brazil (C. M. Gomes). A detailed description of BSM obtained from control and BPH patients was published previously (20).

DNA affinity column chromatography. We used DNA affinity column chromatography as described previously (23) to identify transcription factors that are recruited to the murine CPI-17 promoter. PCR-amplified murine CPI-17 promoter regions were end labeled using T4 polynucleotide kinase and coupled to cyanogen bromide-activated Sepharose 4B as described previously (24) to produce the affinity column. Nuclear proteins from sham-operated and PBOO murine BSM tissue were prepared as described previously (25) for CPI-17 DNA affinity column chromatography. Approximately 1 mg of nuclear protein was loaded per DNA-Sepharose column as described previously (23), and the DNA-bound proteins were eluted with elution buffer containing increasing concentrations of KCl (0.5, 1.0, 1.5, and 2 M KCl). The eluted fractions were assayed for GATA-6 and NF-κB binding to their consensus DNA oligonucleotides by transcription factor enzyme-linked immunosorbent assay (TF-ELISA) according to the manufacturer's instructions (Active Motif, Carlsbad, CA). Immunoblot analysis with antibody to nuclear p97 indicated that this protein represented 1% of the total protein loaded onto the CPI-17 promoter DNA affinity column.

DNA-protein binding by EMSA. The electrophoretic mobility shift assay (EMSA) was performed using a chemiluminescence EMSA kit (Affymetrix, Santa Clara, CA) according to the manufacturer's protocol. The binding reaction mixture contained 5′-end biotin-labeled, double-stranded oligonucleotide probe from the CPI-17 promoter (GATA motifs, −1220 to −1270, or κB motif, −920 to −950), which was purified by column chromatography, and nuclear extract from murine BSM tissue prepared as described previously (25). The binding assay was carried out as described previously (26) using 15 μg of nuclear extract and 10 fmol biotin-labeled oligonucleotide probe. Competition for DNA binding was performed using a 100-fold excess of unlabeled self-oligonucleotides (27). The reaction mixture was preincubated with competitor DNA for 15 min at 25°C prior to the addition of the labeled oligonucleotide probe. For antibody supershift assays, preimmune IgG or antibody specific for GATA-6, NF-κB p50, or c-Rel was added to the reaction mixture and incubated for 20 min on ice before incubation with the biotin-labeled oligonucleotide probe. Samples were electrophoresed on 6% nondenaturing polyacrylamide gels in 0.5× Tris-boric acid-EDTA (1× Tris-boric acid-EDTA is 89 mM Tris base, 89 mM boric acid, and 2 mM EDTA) at 160 V for 1.5 h and transferred to a nylon membrane. The biotin-labeled DNA was visualized using a chemiluminescence method according to the manufacturer's instructions (Affymetrix).

ChIP. Chromatin immunoprecipitation (ChIP) assays were performed on smooth muscle tissues from normal and PBOO mouse bladders as described previously (28). Chromatin samples (200 to 600 bp) were immunoprecipitated overnight at 4°C with antibodies specific for NF-κB p50, c-Rel, or GATA-6 (Abcam, Cambridge, MA) or normal rabbit IgG (Santa Cruz Biotechnology, Santa Cruz, CA) using protein G magnetic beads. The beads were collected and the DNA was eluted as described previously (28). As an input control, an aliquot of sheared chromatin was purified using the QIAquick PCR purification kit (Qiagen, Valencia, CA). All samples were treated with proteinase K (1 mg/ml) for 1 h and subjected to PCR. The PCR products were separated by agarose gel electrophoresis, DNA band intensities were quantified, and the data were analyzed by normalization to the corresponding input values.

RNA extraction and reverse transcription (RT)-PCR. RNA was extracted from BSM tissue devoid of mucosa and serosa and from cultured BSM cells using TRIzol reagent (Invitrogen, Carlsbad, CA) according to the manufacturer's protocol. cDNA synthesis was carried out using standard procedures. The primers used in this study are listed in Table 1.

Protein extraction, coimmunoprecipitation, and immunoblot analysis. Murine bladder muscle tissue devoid of mucosa and serosa was frozen in liquid nitrogen and pulverized into a fine powder. Protein was extracted and analyzed by Western blotting as previously described (29). Briefly, total protein from each sample was separated by sodium dodecyl sulfate-polyacrylamide gel electrophoresis (SDS-PAGE) and transferred to polyvinylidene difluoride membranes (Millipore, Bedford, MA). The membrane was subjected to immunoblot analysis using rabbit polyclonal anti-CPI-17 antibody (United States Biological, Swampscott, MA), and immunoreactive proteins were visualized as described previously (29).

TABLE 1 Primers used in the study

Primer specificity	Primer sequence (5′–3′)	
	Forward	Reverse
Mouse GAPDH	CCACTGAAGGGCATCTTGGGCTAC	CACCACCCTGTTGCTGTAGCC
Human GAPDH	TATTGTTGCCATCAATGACC	GCCAGCATCGCCCCACTTGA
Murine CPI-17 mRNA	ACGAGGTCAACATCGATGAGCTATTG	GGTCATCTGAGGGGCTGGGCT
Human CPI-17 mRNA	GCTGCAGTCTCCATCGCGGG	CATGTCTGCCTCCATGCCGC
Mouse NF-κB p50	GGATAGTGACAGCGTCTGTGACA	ACAGTGTGGGGGAACGGCCA
Human NF-κB p50	GAGGGAGAGCCCACCCGCGC	GGGCCATCTGCTGTTGGCAGT
Mouse GATA-6	TGTACCAGACCCTCGCCGCC	TAGGGCAGGCCGGACAGCAT
Human GATA-6	TGGTGCTTGCCGAAGCGCTTCGGG	CGTGTCGAGCTGAGGCGTCC
Human NF-κB c-Rel	GACTGCGGCCGCCTCCGGCC	GCCTGCTGATCGCCCTTCACA
Murine NF-κB c-Rel	GCCTCGGGCCGGACGCTGGA	TGCGCTCCCCTGGGATGCTA

Equal loading was confirmed by probing the membranes with anti-glyceraldehyde-3-phosphate dehydrogenase (anti-GAPDH) antibody (Abcam). Nuclear extracts were prepared from mouse BSM and primary BSM cells as described previously (30), and immunoblot analysis was carried out as described previously (29) using antibodies specific for NF-κB p50 (Santa Cruz Biotechnology), c-Rel (Abcam), GATA-6 (Abcam), and p97 (RDI Research Diagnostics, Flanders, NJ). Coimmunoprecipitation was performed as described previously (31). For CPI-17 phosphorylation studies, murine BSM tissues from resting and stimulated conditions were rapidly frozen in liquid nitrogen and homogenized in a homogenization buffer containing 1% SDS, 10% glycerol, and 1 mM dithiothreitol (DTT). The proteins were subjected to SDS-PAGE gel electrophoresis and immunoblotted with antibodies against CPI-17 and phospho-CPI-17 (Santa Cruz Biotechnology).

GATA-6 gene silencing by RNA interference. Endogenous expression of GATA-6 was silenced by transient transfection as described previously (20), using predesigned small interfering RNA (siRNA) lentivirus particles for mouse GATA-6 (sc-37908-V) and scrambled siRNA (sc-108080; Santa Cruz Biotechnology). Transfection experiments were performed according to the manufacturer's instructions, and total cell lysates were analyzed for knockdown of GATA-6 mRNA and protein by RT-PCR and immunoblot analysis, respectively. A parallel set of transfected cells was used for ChIP assays. In cotransfection experiments, the CPI-17 promoter reporter plasmid was introduced into BSM cells together with the GATA-6 siRNA.

NF-κB KO mice. NF-κB p50 knockout (KO) mice and the NF-κB cRel KO breeding colony were provided by Christopher Hunter (Department of Pathobiology, University of Pennsylvania, PA). The NF-κB cRel mice were originally from Hsiou-Chi Lieu, Division of Immunology, Department of Medicine, Weill Medical College of Cornell University, NY.

Immunohistochemistry and confocal microscopy. Frozen 5-μm sections of BSM tissue from normal and PBOO mice and from healthy and BPH-induced human bladder were mounted on glass slides. Immunofluorescence staining was performed as described previously (32). Smooth muscle-specific markers SM22 and myosin heavy chain were used to determine the smooth muscle-specific localization of proteins in murine and human bladders, respectively. The primary antibodies used were anti-rabbit CPI-17 (United States Biological), anti-rabbit RhoA (Sigma-Aldrich), anti-rabbit ROCKβ (Sigma-Aldrich), anti-rabbit NF-κB p50 (Santa Cruz Biotechnology), anti-mouse smooth muscle myosin heavy chain (Sigma-Aldrich), and anti-goat SM22 (Abcam). The secondary antibodies used were anti-rabbit Cy3-conjugated and anti-mouse and anti-goat Alexa Fluor 488-conjugated antibodies (Invitrogen). All samples were mounted using VectaShield mounting medium (Vector Laboratories, Inc., Burlingame, CA). High-resolution laser scanning fluorescence microscopy was performed at room temperature using a confocal microscope (Fluoview FV 1000; Olympus) and a 60× oil immersion, numerical aperture 1.45 lens. Images were captured as single acquisitions or as series of time-lapse Z stacks using Fluoview FV10-ASW software (Olympus) and imported into Image J (National Institutes of Health) using LOCI Bio-Formats for Image J. Cy3 fluorescence emission appears red, and fluorescein isothiocyanate (FITC) fluorescence emission appears green. The nuclei were stained with 4′,6′-diamidino-2-phenylindole (DAPI) and assigned to appear blue.

Force measurements. Longitudinal muscle strips (2 by 5 mm) devoid of mucosa and serosa were obtained from wild-type (WT) and NF-κB c-Rel KO mice and suspended in 7 ml of Tyrode's buffer (124.9 mM NaCl, 2.5 mM KCl, 23.8 mM $NaHCO_3$, 0.5 mM $MgCl_2$, 0.4 mM NaH_2PO_4, 1.8 mM $CaCl_2$, 5.5 mM dextrose) in an organ bath (Radnoti) to equilibrate for 1 h in 95% O_2 and 5% CO_2. The force generated in response to KCl (125 mM), electrical field stimulation (80 V, 32 Hz for 1 ms), phorbol dibutyrate (PDBu; 1 μM), and carbachol (10 μM) was measured using the AD Instruments PowerLab computerized system (AD Instruments) as described previously (33, 34). The force measurements were normalized to the wet weight of the muscle strips.

Contraction of permeabilized murine BSM. The BSM was permeabilized and contracted according to the protocol of Stanton et al. (35), with minor modifications. All experiments were performed at room temperature, pH 6.8, and an ionic strength of 120 mM. The composition of all calcium-contracting solutions was calculated using a computer program as previously described (36, 37). Unless otherwise noted, all solutions contained 1 mM Mg^{2+}, 4 mM MgATP, 1 mM DTT, 5 mM EGTA, 20 mM imidazole (pH 6.8), 20 mM creatine phosphate, sufficient K-acetate to maintain the ionic strength constant, and sufficient $CaCl_2$ to achieve the required free [Ca^{2+}]. For membrane permeabilization with alpha-toxin, the muscle strips were treated for 60 min at 25°C with 20 μg ml^{-1} purified *Staphylococcus aureus* alpha-toxin (List, Campbell, CA) at pCa 7.5 buffered with 10 mM EGTA and treated with the Ca^{2+} ionophore A23187 (10 μM; Sigma-Aldrich) for 30 min at 25°C to deplete the sarcoplasmic reticulum Ca^{2+} and maintain constant cytoplasmic Ca^{2+}. The permeabilized bladder smooth muscle strips were initially stimulated at pCa 7.5. When the force reached steady state, the strips were exposed to pCa 7.5 containing 10 μM GTP and 10 μM carbachol, and the force was allowed to develop. The force generation of the muscle strips in response to carbachol was determined by normalization to the maximal force of the muscle strip at pCa 4.5. The effect of PDBu on Ca^{2+} sensitivity was examined in submaximal calcium (pCa 7.5) in the absence of PDBu, followed by stimulation at the same calcium concentration in the presence of PDBu. Ca^{2+} sensitivity was determined by normalizing the force at pCa 7.5 to the maximum response of the muscle strips at pCa 4.5.

Analysis of MLC phosphorylation. MLC phosphorylation in muscle strips was measured as described previously (34). Strips were frozen rapidly at rest (with no stimulation) or at peak force in response to PDBu stimulation by clamp-freezing in liquid N_2 followed by immersion in dry ice-acetone slurry and were stored in liquid nitrogen. Frozen muscle strips were pulverized while immersed in liquid nitrogen, and the resulting powder was added to a mixture of dry ice-acetone. The acetone was removed by centrifugation, and the pellet was mixed with isoelectric focus-

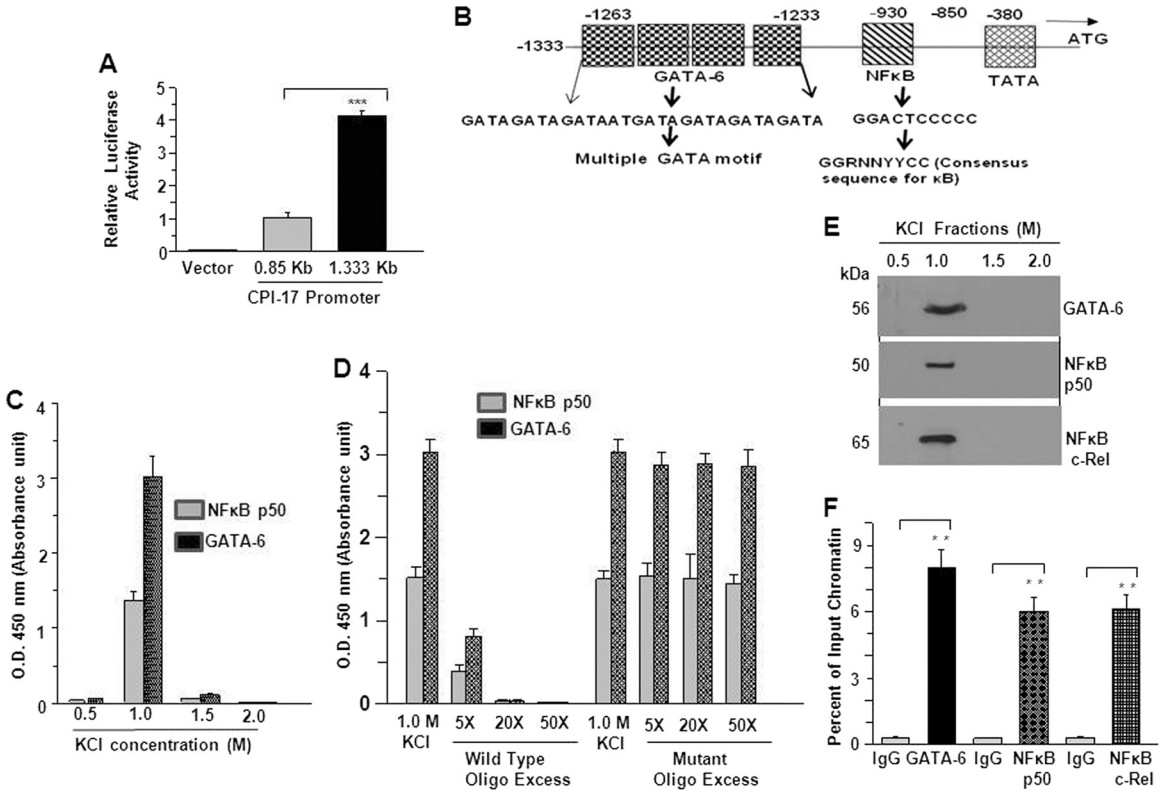

FIG 1 GATA-6 and NF-κB are recruited to the promoter. (A) Mapping the promoter and regulatory regions of the CPI-17 gene. 5′ upstream nucleotide sequences (0.85 kb or 1.333 kb) of the CPI-17 gene were fused to the luciferase reporter (PGL4.1 basic vector) and tested in transient expression assays in murine primary BSM cells. The firefly luciferase activities of the constructs were normalized to *Renilla* luciferase activity. Values are means ± standard deviations (SD) of the results of four independent transfection assays. ***, $P < 0.001$. (B) Schematic representation of the murine CPI-17 promoter. Structural details and putative transcription factor binding sites are shown. The horizontal arrow denotes the direction of transcription. (C) DNA affinity column chromatography. Protein fractions eluted from the DNA affinity column (bp −850 to −1333 region of the CPI-17 promoter) with various KCl concentrations were assayed by TF-ELISA. Binding of NF-κB p50 and GATA-6 to their consensus oligonucleotides was expressed as absorbance units at 450 nm (O.D., optical density). Data are representative of at least three independent triplicate experiments. (D) Oligonucleotide (Oligo) competition assay. Increasing amounts of WT or mutant NF-κB and GATA-6 binding consensus DNA sequence were added to the ELISA plate. (E) Immunoblot analysis of protein fractions bound to CPI-17 promoter. Purified fractions from the DNA affinity column (bp −850 to −1333 region of CPI-17 promoter) were analyzed by immunoblotting. GATA-6, NF-κB p50, and NF-κB c-Rel were detected in the fraction eluted with 1 M KCl. (F) ChIP analysis. Chromatin samples prepared from murine BSM were immunoprecipitated with anti-p50, -c-Rel, and -GATA-6 antibodies or preimmune rabbit IgG as a negative control. Precipitated fragments were PCR amplified using primers specific for κB and GATA motifs of mouse CPI-17 promoter. Quantified band intensities from the agarose gel are presented as percentages of input chromatin. Values are averages of six separate experiments using BSM from six mice ($n = 6$; **, $P < 0.01$).

ing (IEF) sample buffer containing 9.5 M urea, 1.6% ampholyte (pH 5 to 7), 0.4% ampholyte (pH 3 to 10), 2% NP-40, and 5% β-mercaptoethanol and homogenized with a mini-electric homogenizer. After centrifugation, the supernatant was applied to IEF gels, IEF was carried out at 350 V overnight, and gels were subjected to 14% SDS-PAGE and stained with Coomassie blue.

Identification and measurement of MLC phosphorylation using two-dimensional (2-D) gel electrophoresis was performed as described previously (34). Briefly, the identity of these spots in 2-D PAGE was confirmed by Western blotting with an anti-MLC_{20} monoclonal antibody and using pure ^{32}P-phosphorylated myosin. When ^{32}P-phosphorylated myosin was added to the frozen powder, approximately 95% was recovered in the phosphorylated MLC_{20} spots. Spots corresponding to phosphorylated and unphosphorylated MLC_{20} in 2-D PAGE were scanned and analyzed with a Bio-Rad GS-700 imaging densitometer and the 2D-PAGE Molecular Analyst software program (Bio-Rad, Hercules, CA).

Statistical analysis. Where appropriate, comparisons between experimental groups were performed using Student's *t* test. We used one-way analysis of variance from GraphPad Prism software for multiple sample comparisons. A *P* value of <0.05 was considered statistically significant.

RESULTS

Structural features of CPI-17 5′-flanking sequence and its promoter activity. The Bioinformatics tool MatInspector (38) identified a TATA box in the mouse CPI-17 promoter (see Fig. S1 in the supplemental material) but not in the rat or human promoter. The TATA box in mouse CPI-17 promoter is surrounded by the transcription start site (TSS) and a number of GC-rich sequences (GC box). The sequences around the predicted TSS are rich in pyrimidine residues. Comparison of CPI-17 promoter sequences of human, mouse, and rat using ClustalW, a multiple-sequence-alignment computer program (21), revealed a high degree of homology in some regions and variation in others (see Fig. S1). The TSS and GC box sequences in the CPI-17 promoters are well conserved in mouse, rat, and human (see Fig. S1). The GATA motifs are conserved in human, rat, and mouse CPI-17 promoters, although they are present in a different location in the rat promoter (see Fig. S1). Similarly, the κB motif is present in the CPI-17 promoter of all three species but in a different location in each pro-

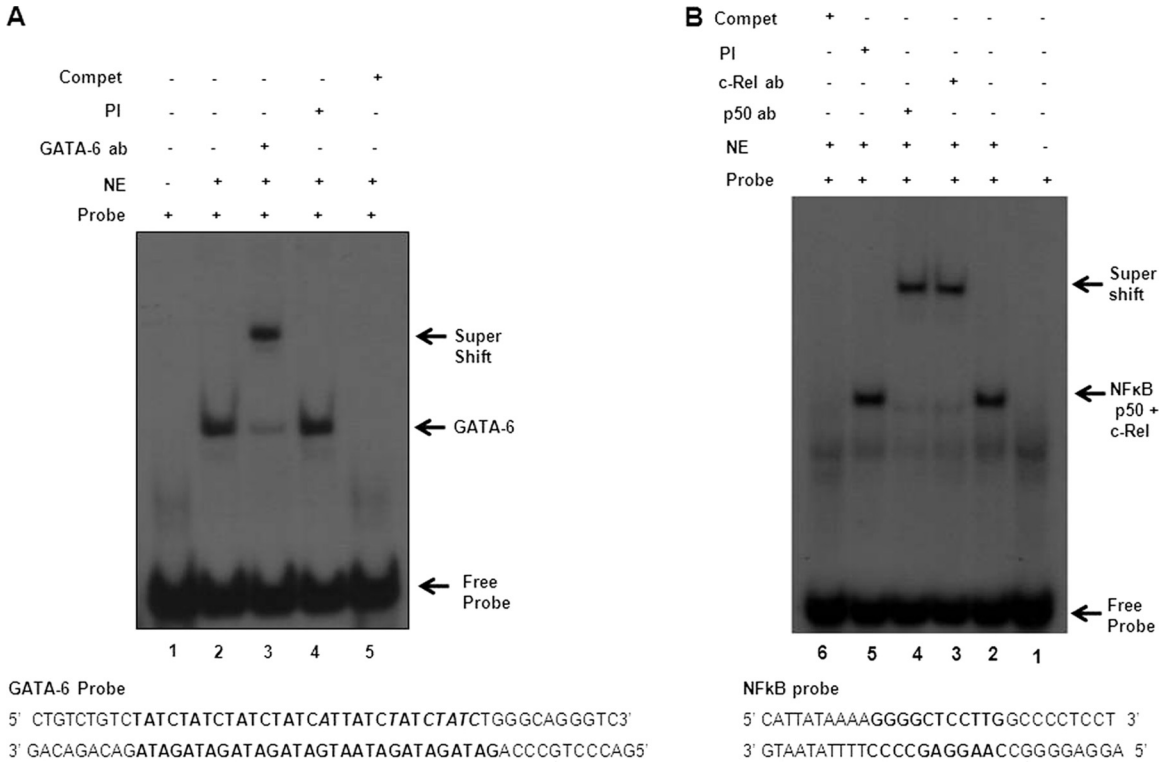

FIG 2 GATA-6 and NF-κB bind to CPI-17 promoter. Gel mobility shift assay was performed using 10 fmol 5′-end biotin-labeled double-stranded oligonucleotide probe from CPI-17 promoter (GATA motifs −1220 to −1270 and κB motif −920 to −950) and 15 μg nuclear extracts (NE) from murine BSM. The reaction mixture was preincubated with the indicated antibodies (ab) or rabbit preimmune (PI) IgG for 20 min on ice before the addition of the labeled DNA probe. Competitor (Compet) containing 100-fold excess of unlabeled self-oligonucleotide was added to the binding reaction mixture 15 min prior to the addition of labeled probe. The migration positions of the free probe, the specific GATA-6, NF-κB p50, and c-Rel DNA complexes, and the supershifted complexes (arrows) are indicated. The boldface letters in the probe sequences indicate the putative GATA-6 and NF-κB binding nucleotides.

moter. To study the promoter activity of the predicted murine CPI-17 promoter, we transfected murine BSM cells with pGL4.1 basic plasmid containing a 1.333-kb DNA fragment representing the genomic sequence from bp +1 to −1333 in the sense orientation. Deletion of 483 bp (−1333 to −850) from this fragment resulted in an approximately 3-fold decrease in luciferase activity in murine BSM cells (Fig. 1A), suggesting a positive *cis* regulatory element within this region. The use of bioinformatics tools revealed multiple GATA motifs and one consensus κB motif in this region (Fig. 1B) and showed that these motifs resemble binding sites for GATA-6 and NF-κB, respectively (Fig. 1B).

GATA-6 and NF-κB are recruited to the CPI-17 promoter. A promoter pulldown method (23) was used to identify transcription factors that interact with the 483-bp (−1333 to −850) region of the CPI-17 promoter. We purified DNA-binding proteins from murine BSM nuclear extract by CPI-17 promoter (bp −1333 to −850) affinity column chromatography. Since structural analysis of the positive *cis* regulatory element (bp −1333 to −850) of the CPI-17 promoter predicted putative binding sites for GATA-6 and NF-κB transcription factors, we specifically tested the purified fractions for the presence of these factors by TF-ELISA and immunoblotting. In addition, the purified fractions were subjected to SDS-PAGE to identify additional transcription factors that bound to the CPI-17 promoter. The fractions eluted with buffer containing 1 M KCl contained GATA-6, NF-κB p50, and c-Rel, as shown by TF-ELISA (Fig. 1C and D) and immunoblotting (Fig. 1E). Excess concentrations (5×, 20×, and 50×) of wild-type but not mutant (at GATA and GGACTCCC sequences) consensus oligonucleotides competed with the oligonucleotide sequence immobilized on the plate for binding to GATA-6 and NF-κB p50 in the TF-ELISA. Fractions eluted with buffer containing 0.5, 1.0, 1.5, and 2.0 M KCl did not contain GATA-4 and GATA-5 as determined by immunoblotting and failed to show any other protein bands, including the NF-κB family member p65, on SDS-PAGE (data not shown).

The *in vitro* binding of GATA-6 and NF-κB to the CPI-17 promoter in murine BSM was confirmed by ChIP assays. Chromatin samples prepared from BSM tissue were precipitated with GATA-6, NF-κB p50, and c-Rel antibodies and subjected to PCR amplification of the GATA-6 and κB consensus motifs in the promoter. Samples immunoprecipitated with anti-GATA-6, -p50, and -c-Rel antibodies yielded prominent PCR products; however, samples immunoprecipitated with preimmune rabbit IgG failed to yield any PCR products. The relative intensities of the bands are reported as the percentages of input chromatin (Fig. 1F).

GATA-6 specifically binds to the conserved GATA motifs in the CPI-17 promoter. A gel shift assay was used to assess the binding of endogenous GATA-6 from BSM nuclear extract to GATA motifs of the CPI-17 promoter (Fig. 2A). A double-stranded, biotin-labeled oligonucleotide corresponding to the CPI-17 promoter GATA motifs (−1220 to −1270) was used as a probe. Nuclear extract from murine BSM formed one major com-

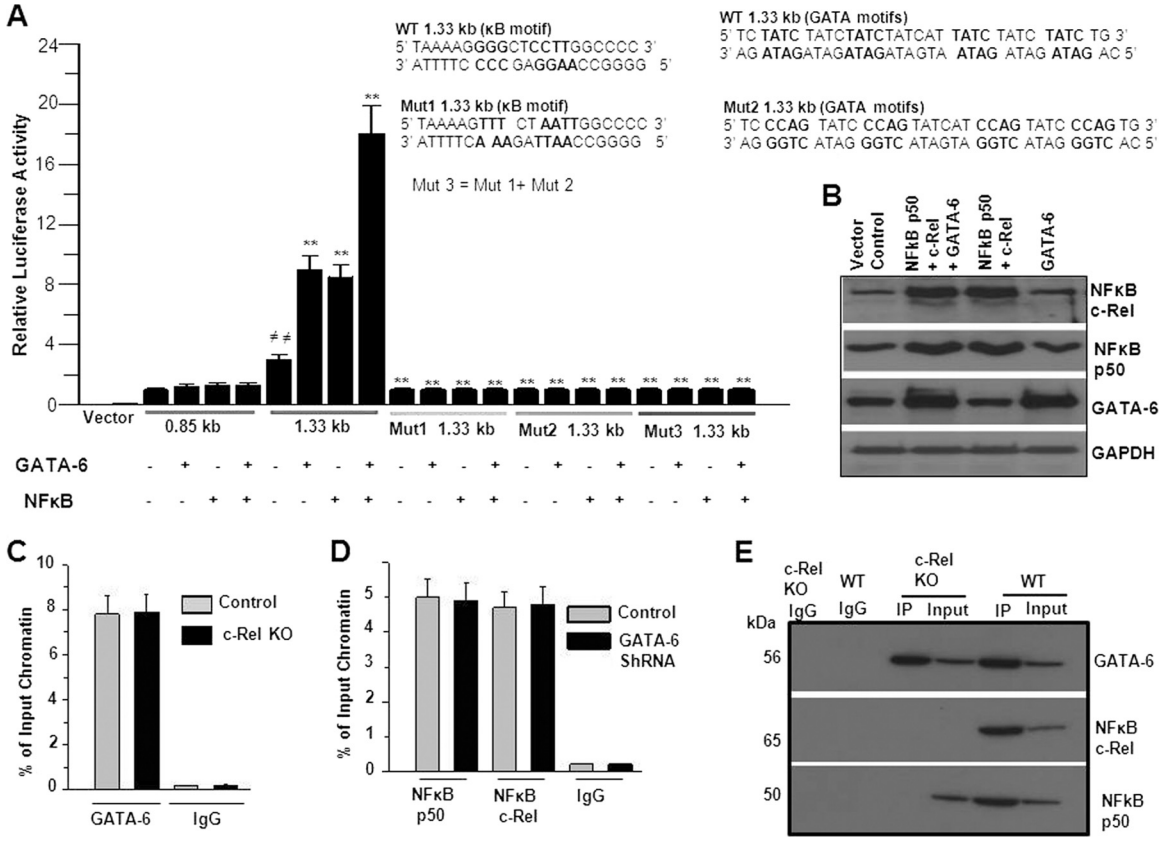

FIG 3 Transcriptional activation of CPI-17 promoter by GATA-6 and NF-κB in primary BSM cells. (A) Murine BSM cells were cotransfected with murine WT or mutant CPI-17 promoter luciferase constructs and GATA-6, NF-κB p50, and c-Rel cDNA. The NF-κB binding site (κB motif) mutation in the 1.33-kb CPI-17 promoter is designated Mut1. The GATA-6 binding site (multiple GATA motifs) mutation is designated Mut2. The double mutant with both Mut1 and Mut2 mutations is designated Mut3. Mutant nucleotides are shown in boldface font. Luciferase activity was measured in each sample after 72 h and is presented relative to that of *Renilla* luciferase. Data are presented as means ± SD from five independent experiments. ≠≠, $P < 0.01$ compared with results for 0.85-kb CPI-17 promoter; **, $P < 0.01$ compared with results for 1.33-kb CPI-17 promoter. (B) Representative immunoblot showing the expression levels of ectopically expressed GATA-6, NF-κB p50, and c-Rel compared with their endogenous levels. (C and D) ChIP analysis of CPI-17 promoter in WT and c-Rel KO murine BSM with GATA-6 antibody ($n = 5$) (C) and of CPI-17 promoter in scrambled (Control) and GATA-6 shRNA knockdown BSM cells with NF-κB p50 and c-Rel antibodies (D). GATA motifs (C) and κB motif (D) in the murine CPI-17 promoter were amplified by PCR. Preimmune serum (IgG) was used as a negative control in both ChIP experiments. Data are presented as the means ± SD of five experiments. (E) Coimmunoprecipitation of GATA-6, NF-κB p50, and c-Rel in WT and c-Rel KO mouse BSM. Immunoprecipitates from WT and c-Rel KO murine BSM nuclear extracts by GATA-6 antibody were subjected to immunoblot analysis with GATA-6, NF-κB p50, and c-Rel antibodies. An immunoblot representative of five different experiments is presented ($n = 5$).

plex with the GATA oligonucleotide probe (Fig. 2A, lane 2). This DNA protein complex was supershifted by anti-GATA-6 antibody (Fig. 2A, lane 3) whereas preimmune serum did not yield any detectable supershift (Fig. 2A, lane 4). Furthermore, the DNA-protein complex formed with the GATA oligonucleotide probe was effectively competed by excess unlabeled self-oligonucleotides (Fig. 2A, lane 5). These experiments demonstrated specific binding of endogenous GATA-6 to GATA motifs in the CPI-17 promoter.

NF-κB p50 and c-Rel specifically bind to the conserved κB motif in the CPI-17 promoter. Binding of endogenous NF-κB from murine BSM nuclear extract to the κB motif of the murine CPI-17 promoter was investigated by EMSA. An oligonucleotide probe containing the NF-κB binding site (−920 to −950 of the murine CPI-17 promoter) formed a single DNA protein complex with murine BSM nuclear extract (Fig. 2B, lane 2). This DNA-protein complex was supershifted by the addition of NF-κB p50 and c-Rel antibodies (Fig. 2B, lanes 3 and 4), whereas preimmune serum did not yield any detectable supershift (Fig. 2B, lane 5). The addition of a 100-fold molar excess of unlabeled κB binding oligonucleotide to the reaction mixture abolished DNA-protein complex formation (Fig. 2B, lane 6), demonstrating the specificity of this motif for NF-κB p50 and c-Rel.

GATA and κB motifs of the CPI-17 promoter recruit GATA-6 and NF-κB. Cotransfection of murine BSM cells with the 1.333-kb CPI-17 promoter reporter construct and either GATA-6 or NF-κB cDNA resulted in activation of the 1.333-kb promoter, whereas no activation of the 0.85-kb promoter was detected (Fig. 3A), suggesting that GATA-6 and NF-κB are recruited to the 483-bp region within the 1.333-kb promoter. The expression levels of exogenously expressed GATA-6 and NF-κB compared with the levels in the control are shown in Fig. 3B. Transfection analysis of the 1.33-kb CPI-17 promoters Mut1, Mut2, and Mut3 in murine BSM demonstrated that mutation of the GATA and κB motifs (separately or in combination) reduced promoter activity to the basal level, equivalent to that of the 0.85-kb CPI-17 promoter. Thus, both GATA and κB motifs are required for GATA-6- and NF-κB-mediated transcriptional activation of the 1.33-kb CPI-17

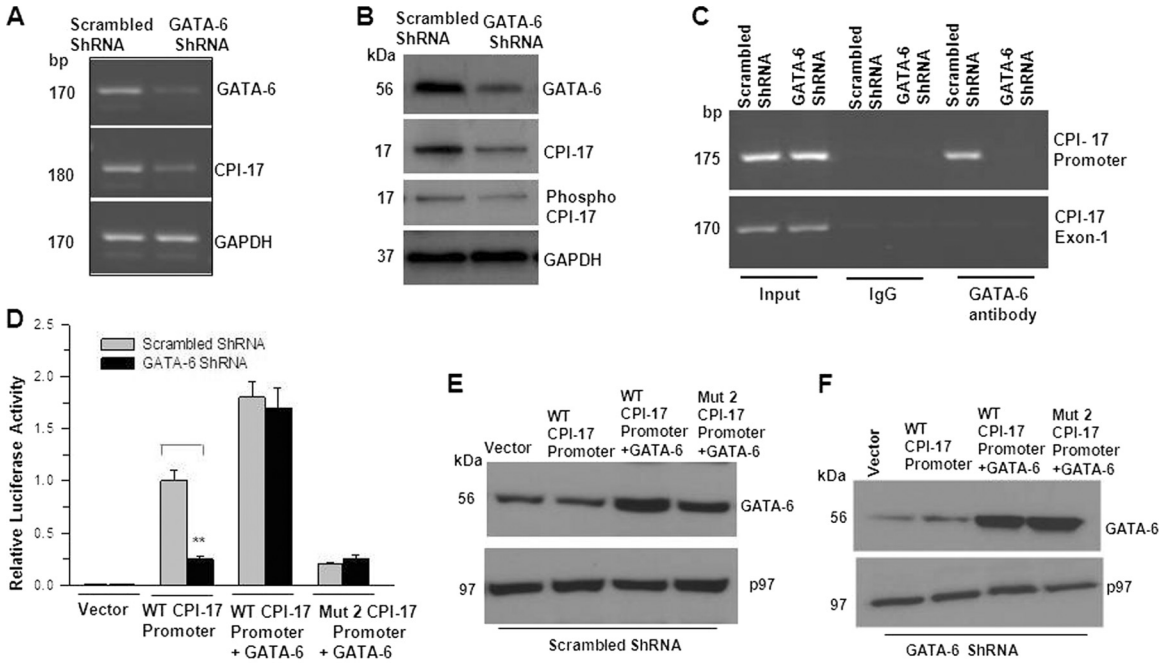

FIG 4 Silencing of GATA-6 downregulates CPI-17 gene expression. (A and B) RT-PCR (A) and immunoblot analysis (B) of GATA-6 and total and phosphorylated CPI-17 in murine BSM cells transduced with scrambled (control) and GATA-6 shRNA. Representative blots from three different experiments are presented. (C) ChIP analysis of the CPI-17 promoter using GATA-6 antibody in murine BSM cells transfected with scrambled or GATA-6 shRNA. The GATA-6 binding motif in the murine CPI-17 promoter was amplified by PCR. Preimmune serum (IgG) was used as a negative control. (D) Relative luciferase activities in murine BSM cells transfected with scrambled and GATA-6 siRNA. Reporter firefly luciferase activities were normalized to *Renilla* luciferase activity. Data are presented as means ± SD of three independent experiments. **, $P < 0.01$ compared with the results for scrambled shRNA. (E and F) Immunoblot analysis of the expression levels of endogenous GATA-6 and exogenously transfected GATA-6 in scrambled shRNA and GATA-6 shRNA knockdown cells. Representative blots from three different experiments are presented.

promoter. As shown in Fig. 3A, cotransfection with GATA-6 and NF-κB significantly upregulated CPI-17 promoter activity (6-fold) compared with transfection with either GATA-6 or NF-κB alone (2.5-fold), suggesting that these two transcription factors act additively to activate the CPI-17 gene. Mutations at the κB (Mut1) and GATA (Mut2) motifs of the CPI-17 promoter reporter construct abolished the additive effect of GATA-6 and NF-κB on CPI-17 promoter activation. However, the binding of GATA-6 to the CPI-17 promoter in NF-κB c-Rel KO BSM was equivalent to that in WT BSM (Fig. 3C), and the binding of NF-κB p50 and c-Rel to the CPI-17 promoter was not altered in GATA-6 knockdown cells compared with their binding in the control (Fig. 3D). This suggests that although the activation is additive, each factor is dependent on the presence of both binding sites for activity; the loss of one factor does not affect the binding of the other factor (Fig. 3C and D). To gain further insight into the mechanism of GATA-6 and NF-κB interaction, we examined the interaction between GATA-6 and NF-κB p50 and c-Rel by coimmunoprecipitation studies. Immunoprecipitation of nuclear extracts from WT and c-Rel KO murine BSM with anti-GATA-6 antibody showed that GATA-6 interacts with NF-κB p50 and c-Rel in WT BSM (Fig. 3E). However, GATA-6 failed to interact with NF-κB p50 in the absence of c-Rel (Fig. 3E) suggesting that c-Rel is required for complex formation between these transcription factors. These findings rule out the possibility that an abundance of one transcription factor affects transcription indirectly, for example, by enhancing the expression of the other factor. The additive effect of GATA-6 and NF-κB on CPI-17 promoter activity was also observed in 293T cells (data not shown), suggesting that this phenomenon is not specific to BSM cells.

The expression of CPI-17 mRNA and protein (total and phospho-CPI-17) decreased after knockdown of GATA-6 (Fig. 4A and B). In ChIP experiments, samples immunoprecipitated with anti-GATA-6 antibody from murine scrambled small hairpin RNA (shRNA)-transfected cells yielded prominent PCR products (Fig. 4C, 5th lane), whereas GATA-6 shRNA-transfected cells failed to yield any detectable amplified DNA (Fig. 4C, 6th lane). Similarly, samples immunoprecipitated with preimmune rabbit IgG from scrambled and GATA-6 shRNA-transfected cells did not yield any PCR products (Fig. 4C, 3rd and 4th lanes). Importantly, transfection of GATA-6 shRNA into these cells resulted in the loss of GATA-6 binding to the CPI-17 promoter (Fig. 4C, 6th lane). This correlated with decreased reporter gene activity, which could be rescued by reexpression of GATA-6 (Fig. 4D). The expression levels of exogenously expressed GATA-6 in scrambled (control) and GATA-6 knockdown cells are shown in Fig. 4E and F. These results provide direct proof that transcriptional activation of the CPI-17 gene in murine BSM cells is mediated by recruitment of GATA-6 to GATA motifs in the CPI-17 promoter.

Transcriptional activation of CPI-17 by GATA-6 and NF-κB. Since GATA-6 and NF-κB are recruited to the CPI-17 promoter in murine BSM, we next addressed the effects of GATA-6 and NF-κB overexpression on endogenous CPI-17 gene expression. Murine BSM cells were transfected with NF-κB p50 and c-Rel cDNA as described previously (20). Adenovirus encoding GATA-6 or LacZ was introduced into murine BSM primary cells by transduction.

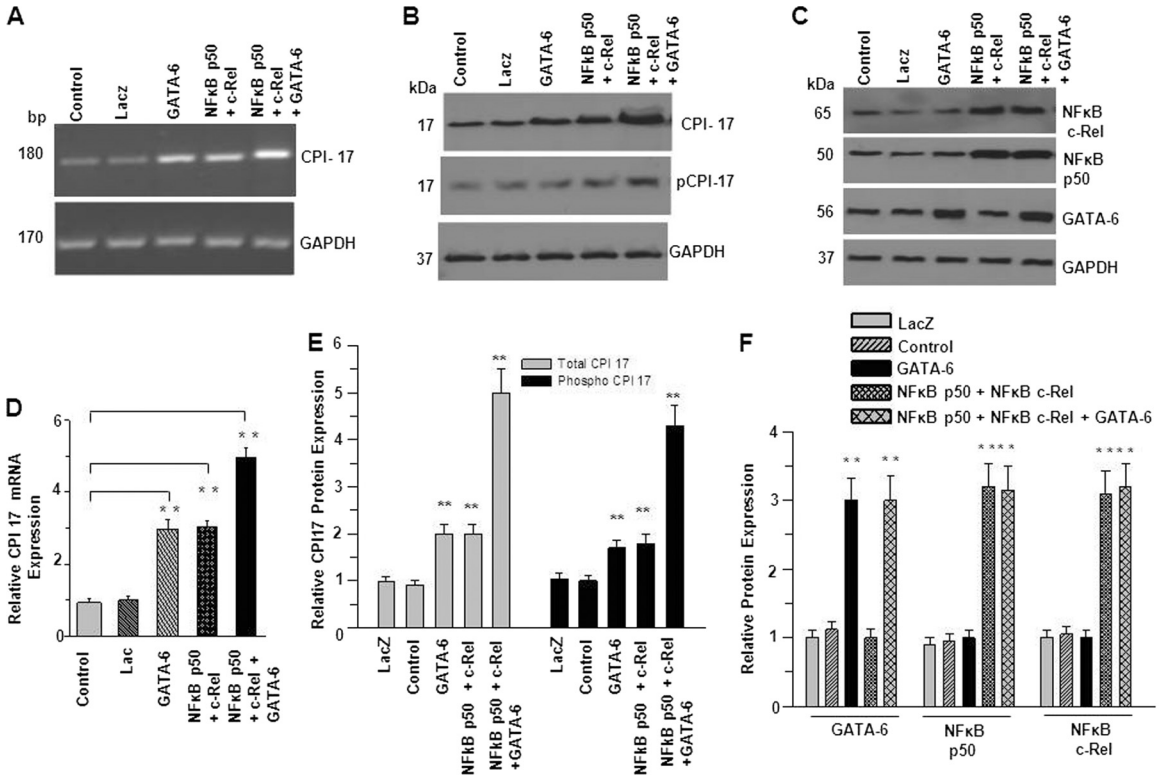

FIG 5 GATA-6 and NF-κB upregulate endogenous CPI-17 expression in primary BSM cells. (A to C) Murine BSM cells were transduced with adenovirus encoding GATA-6, LacZ, or NF-κB p50 and c-Rel cDNA individually and in combination for 72 h. RNA and protein were extracted and subjected to RT-PCR (A) and immunoblot analysis (B and C) for total and phospho-Thr^{38}-CPI-17 (pCPI-17), GATA-6, NF-κB p50, c-Rel, and GAPDH. (D to F) Data from the experiments for which representative results are shown in panels A to C are presented as means ± SD from four independent experiments. **, $P < 0.01$ compared with control.

Overexpression of GATA-6, NF-κB p50, and c-Rel in murine BSM cells increased the levels of endogenous CPI-17 mRNA (Fig. 5A) and of total and phospho-CPI-17 protein (Fig. 5B) relative to the level of LacZ, showing that these factors act as transcriptional activators of CPI-17 gene expression. The expression levels of total CPI-17, phospho-CPI-17, GATA-6, NF-κB p50, and c-Rel in transfected and control cells are shown in Fig. 5C to F.

NF-κB p50 and c-Rel are required for CPI-17 gene expression in murine BSM *in vivo*. We next investigated the effects of NF-κB p50 and c-Rel gene silencing on CPI-17 gene expression. The expression levels of CPI-17 mRNA (Fig. 6A and B) and protein (Fig. 6C and D) decreased significantly in p50 and c-Rel KO BSM compared with their levels in WT BSM. The loss of CPI-17 expression in BSM from c-Rel KO mice was further demonstrated by confocal microscopy (Fig. 6E); similar findings were obtained with BSM from p50 KO mice (data not shown). Together, these findings demonstrate that NF-κB p50 and c-Rel are required for CPI-17 expression in murine BSM. The expression profiles of RhoA and ROCKβ in BSM isolated from WT, NF-κB p50 KO, and c-Rel KO mice revealed that the expression levels of RhoA and ROCKβ proteins were 3-fold greater in BSM from NF-κB c-Rel KO and p50 KO mice than in WT BSM (Fig. 7A to D). Since there is increased expression of ROCKβ in c-Rel KO mouse bladders, we investigated phosphorylation levels of the ROCKβ substrate MYPT in the same tissues. As shown in Fig. 7E, phosphorylation of MYPT1 at both Thr^{696} and Thr^{850} was increased in c-Rel and p50 KO BSM compared with that in WT BSM. However, increased expression of ROCKβ in c-Rel KO BSM was not associated with increased CPI-17 phosphorylation in the same tissues, suggesting that PKC, rather than ROCKβ, plays a major role in CPI-17 phosphorylation in BSM. This is in agreement with an earlier report that the ROCK isoform that phosphorylates MYPT1 is not involved in *in vivo* phosphorylation of CPI-17 in BSM (5, 39).

NF-κB regulates PKC-mediated signaling of smooth muscle contraction. Since CPI-17 is a downstream target of PKC, we analyzed the force generation of PKC-mediated contraction in BSM strips from WT and c-Rel KO mice. Representative force profiles in response to 1 μM PDBu (a PKC agonist) are shown in Fig. 8A. BSM from c-Rel KO mice exhibited significantly lower force generation in response to PDBu than BSM from WT mice (Fig. 8C) ($n = 5$, $P < 0.01$). Preincubation with BIS (*N*,*N*-methylenebisacrylamide), a PKC inhibitor, abolished the PDBu-induced contraction in BSM from WT and c-Rel KO bladders (data not shown). These findings indicate that the transcription factor NF-κB c-Rel is required for PKC-mediated smooth muscle contraction. To determine whether decreased CPI-17 expression affects receptor-independent contraction, we measured the force profiles of BSM from WT and NF-κB c-Rel KO mice in response to 125 mM KCl (Fig. 8B). In our study, the initial Ca^{2+}-dependent phasic contraction was significantly increased in NF-κB c-Rel KO BSM compared with that in WT BSM and was followed by a sharp decline in tonic-phase contractions (Fig. 8B) ($n = 5$, $P < 0.01$). Although the muscle strips from c-Rel KO mouse bladders generated more force (Fig. 8D), force maintenance was lower than that

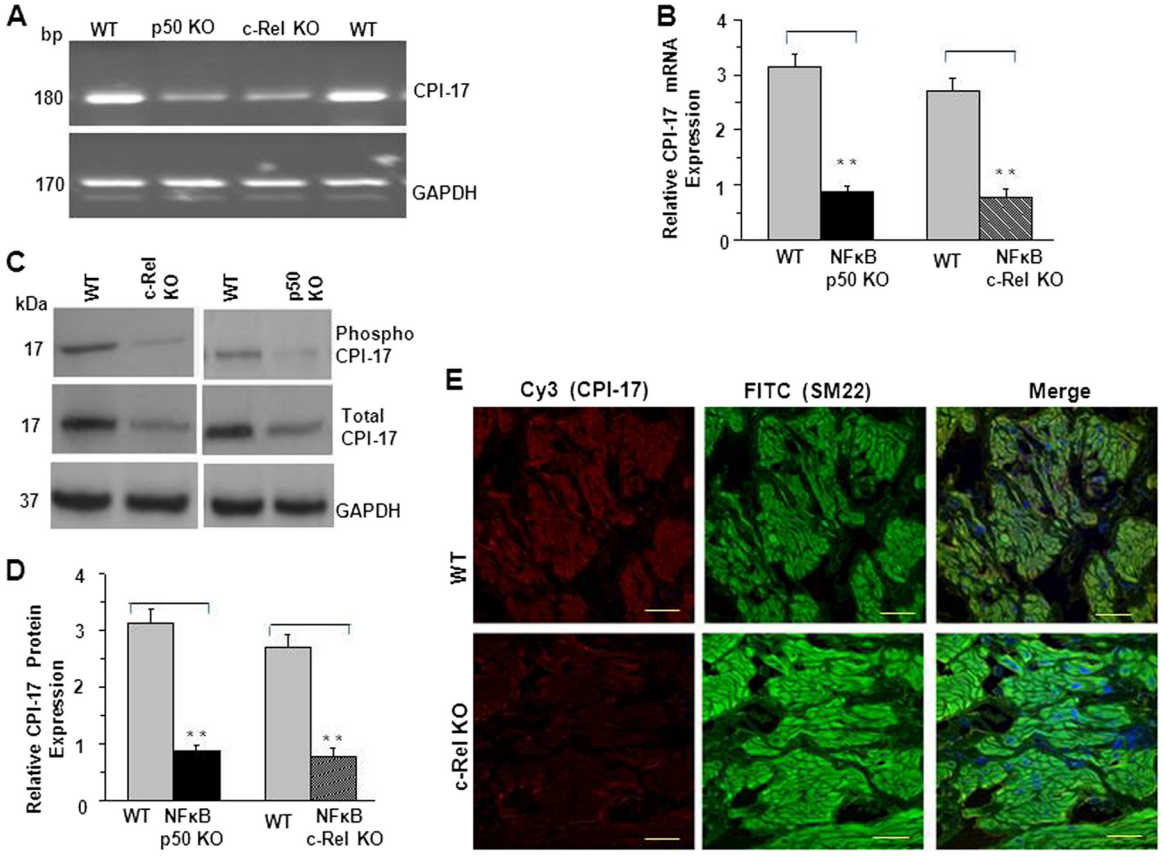

FIG 6 NF-κB silencing downregulates CPI-17 gene expression. RT-PCR (A and B) and immunoblot (C and D) analyses of CPI-17 mRNA and total and phospho-CPI-17 protein in WT, NF-κB p50 KO, and NF-κB c-Rel KO mouse BSM tissues. Data are presented as the means ± SD of five experiments. **, $P <$ 0.01 compared with WT. (E) Immunofluorescence analysis of CPI-17 in WT and c-Rel KO mouse bladders. BSM tissue was stained with anti-CPI-17 and anti-SM22 polyclonal antibody (1:100) followed by Cy3- and FITC-conjugated secondary antibodies. Scale bars = 20 μm. Representative confocal images are presented.

of BSM strips from WT mice (Fig. 8B). It appears that the increased expression of RhoA and ROCKβ and the increased MYPT1 phosphorylation in NF-κB c-Rel KO mouse BSM failed to maintain the contractile force during the sustained slow tonic phase. These results suggest that CPI-17, in addition to RhoA and ROCK, is important for force maintenance during the sustained slow tonic phase of smooth muscle contraction.

Since CPI-17 is a potent inhibitor of MLCP activity, it is likely that reduced CPI-17 expression in c-Rel KO mouse BSM affects the level of MLC_{20} phosphorylation. Therefore, we performed 2-D gel electrophoresis of proteins isolated from muscle strips obtained during PDBu stimulation. Surprisingly, MLC_{20} phosphorylation in c-Rel KO mouse BSM was similar to that of WT mouse BSM at the peak force (Fig. 8E to G). The increased expression of RhoA and ROCKβ in c-Rel KO BSM did have a compensatory effect on maintenance of MLC_{20} phosphorylation in the absence of CPI-17 (Fig. 8G; compare the spots for phosphorylated MLC_{20} and the graph). Together, these observations suggest that the PKC-mediated BSM contraction that occurs through CPI-17 expression in response to agonist stimulation is independent of MLC_{20} phosphorylation, in accordance with earlier observations in rabbit vascular smooth muscle (39, 40).

G protein receptor-dependent BSM contraction and CPI-17 phosphorylation in WT and NF-κB c-Rel KO mouse tissue samples. To investigate whether decreased expression of CPI-17 affects G protein receptor-dependent contraction, we measured force profiles of BSM from WT and NF-κB c-Rel KO mice in response to 10 μM carbachol (Fig. 9A and B). Smooth muscle strips from WT and c-Rel KO mice developed a quick, phasic-like contraction in response to carbachol, after which the force rapidly decreased to maintain a value that was 50% of the maximal force at 4 to 7 min (Fig. 9C) ($n = 6$, $P < 0.01$). There was a loss of force maintenance during the sustained contraction in c-Rel KO BSM compared with that in WT BSM (Fig. 9A to C) ($n = 5$, $P < 0.01$). We next investigated PKC-mediated CPI-17 phosphorylation in WT and c-Rel KO BSM using a phosphorylation site-specific antibody against phospho-Thr^{38}-CPI-17. The levels of phospho-Thr^{38}-CPI-17 increased with carbachol stimulation in both WT and c-Rel KO mice; however, the level of CPI-17 phosphorylation in response to carbachol stimulation was lower in c-Rel KO mice than in WT mice (Fig. 9D). Since PKC-mediated CPI-17 phosphorylation is observed in BSM, we next investigated the effect of c-Rel KO on the expression of PKC isoforms in WT and c-Rel KO mice by immunoblotting (Fig. 9E). There was no difference in the expression of different PKC isoforms between c-Rel KO and WT mice, suggesting that the decreased amount of phospho-CPI-17 in c-Rel KO mice in response to carbachol stimulation is probably due to significant loss of total CPI-17 protein rather than a deficiency of PKC.

To test the effect of decreased CPI-17 expression on calcium sensitization of BSM contraction, we performed the force mea-

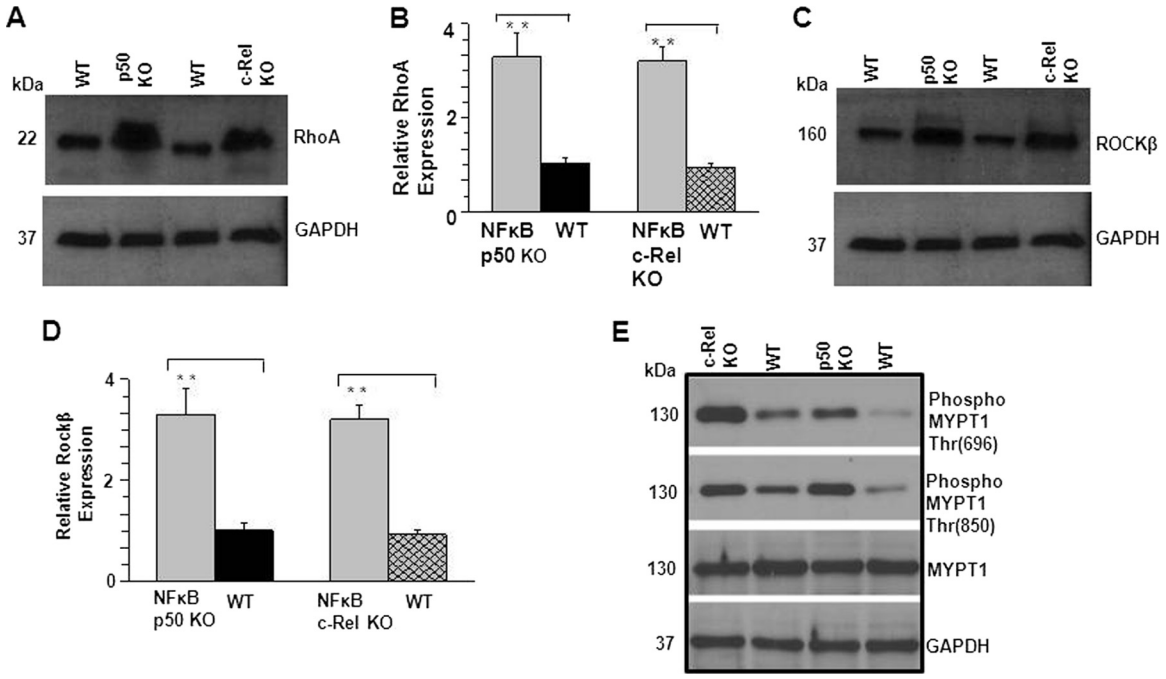

FIG 7 NF-κB silencing upregulates RhoA and ROCKβ expression in murine BSM. (A and C) Immunoblot analyses of RhoA (A) and ROCKβ (C) expression in WT, p50 KO, and c-Rel KO mouse BSM tissue. (B, D) Data are presented as means ± SD of five experiments. **, $P < 0.01$ compared with the results for WT mice. (E) Expression of total MYPT, phospho-Thr^{696}-MYPT1, and phospho-Thr^{850}-MYPT1 in WT, p50 KO, and c-Rel KO BSM tissues. An immunoblot representative of five different experiments is presented.

surements at a constant low free Ca^{2+} concentration (pCa 7.5). Permeabilized muscle strips of WT and c-Rel KO mouse bladder produced higher force in response to carbachol-plus-GTP stimulation than to Ca^{2+} alone at pCa 7.5 (from 7% ± 1% with Ca^{2+} alone to 30% ± 4% with Ca^{2+} plus carbachol plus GTP). These results demonstrate that carbachol plus GTP increases the calcium sensitivity of contractile filaments in both WT and c-Rel KO mouse BSM (Fig. 9F). In alpha-toxin-permeabilized WT BSM, PDBu generated higher force than Ca^{2+} alone at PCa 7.5 (from 5% ± 1% with Ca^{2+} alone to 22% ± 6% with Ca^{2+} plus PDBu) (Fig. 9F). On the other hand, BSM from c-Rel KO mice failed to increase the force in response to PDBu, indicating the loss of calcium sensitization due to decreased CPI-17 expression. Together, these results suggest that CPI-17 is required for PDBu-activated, PKC-mediated calcium sensitization of BSM contraction.

Overexpression of NF-κB p50 and c-Rel correlates with CPI-17 expression in an animal model of PBOO. We previously demonstrated increased expression of GATA-6 in outlet obstruction-induced pathological smooth muscle hypertrophy in mice and humans (20). Therefore, we determined the expression profiles of CPI-17, NF-κB p50, and c-Rel in PBOO-induced BSM hypertrophy. Compared to the results for BSM from control mice, CPI-17, phospho-CPI-17, NF-κB p50, and c-Rel were significantly overexpressed in BSM tissues from PBOO mice both at the mRNA and protein levels (Fig. 10 and 11). Tissue sections from sham-operated and obstructed mouse bladders were stained with anti-NF-κB p50 antibody and examined by confocal microscopy. NF-κB p50 localized to both the nucleus and the cytoplasm of the smooth muscle bundles in sham-operated and PBOO bladders, and its expression was higher in bladders from PBOO mice than in bladders from sham mice (Fig. 12). Increased expression of NF-κB p50 localized within PBOO smooth muscle bundles, as shown by costaining with SM22, a specific marker for smooth muscle.

PBOO-induced remodeling promotes recruitment of GATA-6 and NF-κB to the CPI-17 promoter. Since PBOO induces NF-κB p50, c-Rel, and GATA-6 in murine BSM, we examined the recruitment of these transcription factors to the *CPI-17* promoter in smooth muscle by ChIP. Chromatin samples were prepared from control, sham-operated, and PBOO BSM, precipitated with anti-NF-κB p50, -c-Rel, and -GATA-6 antibodies, and subjected to PCR amplification of the CPI-17 promoter NF-κB and GATA-6 consensus binding motifs. Samples immunoprecipitated with anti-GATA-6 antibody yielded prominent PCR products in PBOO samples (Fig. 13A, 6th lane) compared with the results for sham-operated samples (Fig. 13A, 5th lane); however, samples immunoprecipitated with preimmune rabbit IgG failed to yield PCR products (Fig. 13A, 3rd and 4th lanes). Similarly, samples immunoprecipitated with anti-NF-κB p50 and -c-Rel antibodies yielded prominent PCR products in PBOO (Fig. 13B and C, 6th lanes) compared with the results for sham-operated (Fig. 13B and C, lane 5) mouse bladders, while samples immunoprecipitated with preimmune rabbit IgG failed to yield PCR products (Fig. 13B and C, 3rd and 4th lanes). The relative intensities of the bands shown in Figure 13A to C were determined as percentages of input chromatin (Fig. 13D and E). These data indicate increased binding of GATA-6 and NF-κB to the CPI-17 promoter in PBOO-induced smooth muscle hypertrophy.

BSM remodeling caused by BPH-induced outlet obstruction promotes NF-κB, GATA-6, and CPI-17 gene expression and enhances recruitment of these transcription factors to the CPI-17 promoter. Bladder outlet obstruction is considered one of the

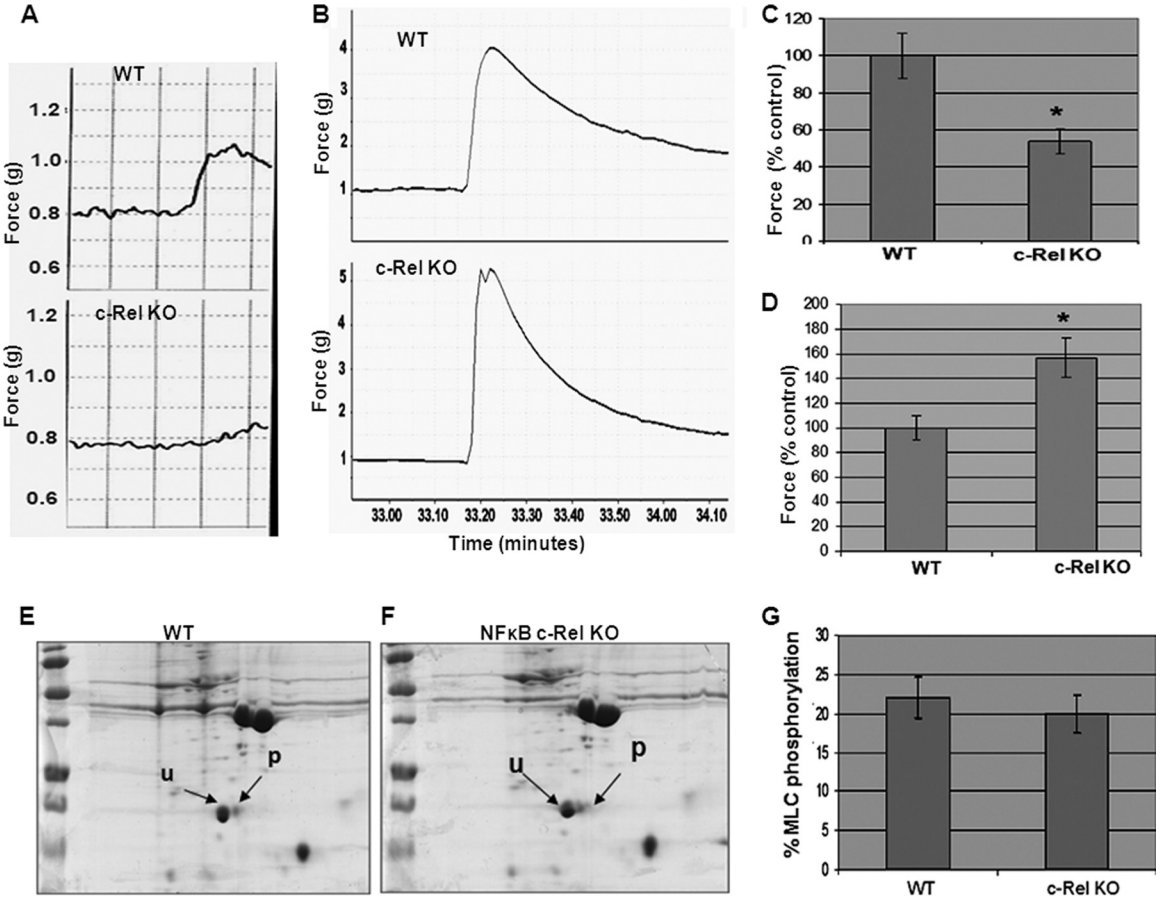

FIG 8 Effects of NF-κB silencing on PKC- and RhoA-mediated BSM contraction. (A and B) Representative force profiles for WT and NF-κB c-Rel KO mouse BSM strips in response to PDBu and KCl. Isolated BSM strips were stretched intermittently while being stimulated with electrical field stimulation (80 V, 32 Hz for 1 ms) to determine optical length (Lo). Individual BSM strips were stimulated with 1.0 μM PDBu, a PKC activator (A), and force was recorded at the peak of contraction. Similarly, the strips were stimulated with 125 mM KCl (B) to determine the maximal contractile response. (C and D) Means of five separate experiments using BSM strips from five WT and five NF-κB c-Rel KO mice stimulated with PDBu (C) ($n = 5$, $P < 0.05$) or KCl (D) ($n = 5$, $P < 0.05$). (E and F) Representative profiles of 2-D gel electrophoresis showing MLC_{20} phosphorylation. Protein extracts were prepared from muscle strips freeze-clamped at the peak of maximal force in response to PDBu. Arrows indicate spots for phosphorylated (p) and unphosphorylated (u) MLC_{20} in Coomassie blue-stained 2-D gels. (G) Quantification of the results from five experiments ($n = 5$) determined by densitometry.

key factors in BPH-induced lower urinary tract symptoms (LUTS) in aged men (41, 42), and it is associated with remodeling and hypertrophy of the BSM that eventually leads to contractile dysfunction (41, 42). PBOO-induced smooth muscle remodeling and hypertrophy are associated with altered expression of contractile, signaling, and regulatory proteins (16, 20, 29, 35, 43–46). Similar to the murine PBOO model, we observed increased expression of NF-κB c-Rel and p50 in BSM from obstructed bladders compared with their expression in bladders from healthy controls (Fig. 14A and B). The expression of NF-κB p50, c-Rel, and GATA-6 in BSM from obstructed bladders was positively correlated with total and phospho-CPI-17 expression (Fig. 14A to E). Analysis of the human CPI-17 promoter identified GATA motifs and one canonical κB motif within a 1-kb region (see Fig. S1 in the supplemental material), reminiscent of binding sites for GATA-6 and NF-κB, respectively. Human BSM cells transiently transfected with human CPI-17 promoter, CPI-17 promoter plus GATA-6, or CPI-17 promoter plus NF-κB showed increased promoter activity (data not shown). Furthermore, cotransfection of human BSM cells with human CPI-17 promoter, GATA-6, and NF-κB cDNA additively induced promoter activity, and this effect was stronger than that induced by individual expression of either of the transcription factors (data not shown). We also observed increased binding of these transcription factors to the CPI-17 promoter in smooth muscle samples from obstructed bladders from BPH patients compared with that in smooth muscle samples of bladders from healthy controls (Fig. 14F). Taken together, these results demonstrate that the transcription factors GATA-6 and NF-κB mediate CPI-17 transcription and provide important information about the molecular mechanism responsible for CPI-17 overexpression during BSM remodeling and hypertrophy associated with BPH-induced LUTS.

DISCUSSION

Our study demonstrates for the first time that the transcription factors GATA-6 and NF-κB activate CPI-17 gene transcription by binding to GATA and κB motifs, respectively, in the CPI-17 promoter. Deficiency in these factors decreases CPI-17 expression, resulting in impairment of smooth muscle contraction. Recently,

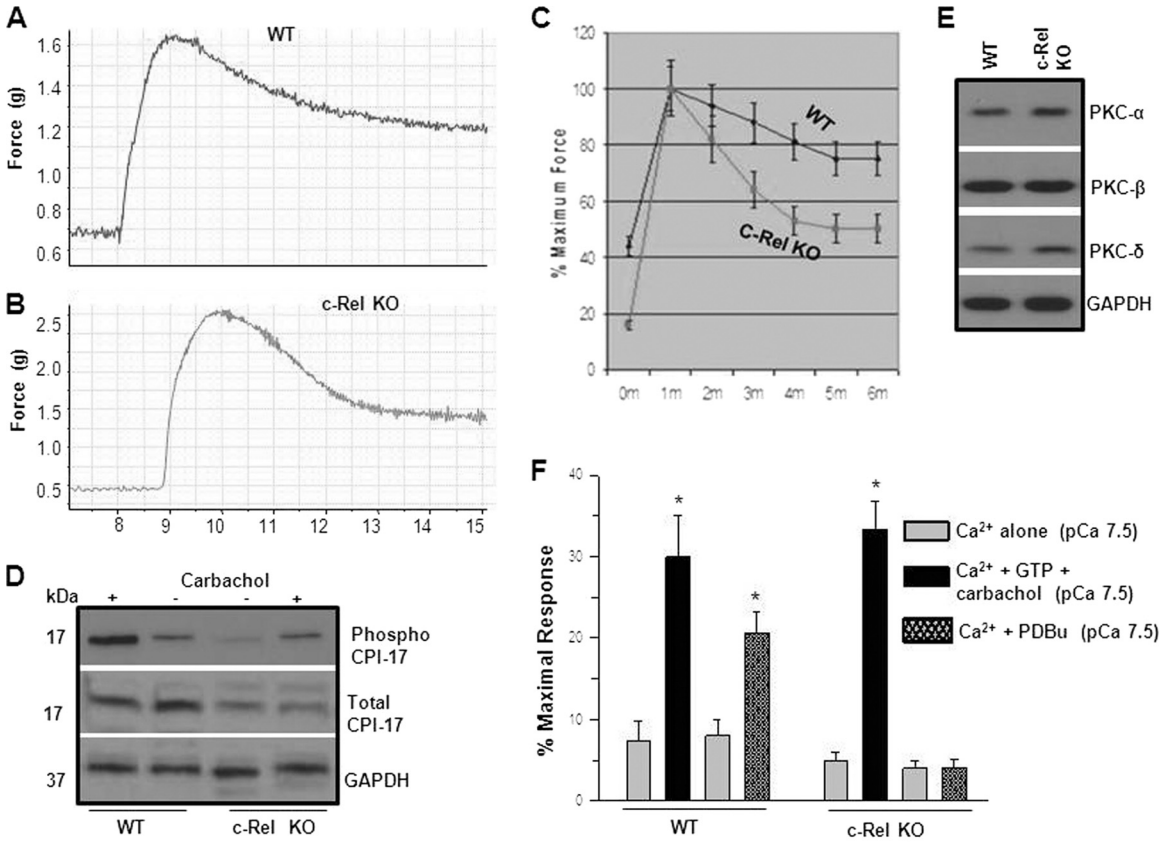

FIG 9 Carbachol-induced BSM contraction in NF-κB c-Rel KO mice. (A and B) Representative force profiles of WT and NF-κB c-Rel KO mouse BSM strips in response to carbachol as a function of time (in minutes). Isolated BSM strips were stretched intermittently while being stimulated with electrical field stimulation (80 V, 32 Hz for 1 ms) to determine optical length (Lo). Individual strips were stimulated with 10 μM carbachol, and force was recorded at the peak of contraction. (C) Quantification of force maintenance in NF-κB c-Rel KO and WT BSM in response to carbachol stimulation. The graph shows the means ± standard errors of the mean of five separate experiments ($n = 5$, $P < 0.05$). (D) Representative immunoblot showing CPI-17 phosphorylation in response to carbachol stimulation in WT and c-Rel KO BSM. Protein extract prepared from muscle strips freeze-clamped at the peak of maximal force in response to carbachol was analyzed by immunoblotting for total and phospho-CPI-17 expression levels. GAPDH was used as a loading control. (E) Immunoblot analysis of PKCα, PKCβ, and PKCδ expression in WT and c-Rel KO mouse BSM. A representative immunoblot from five separate experiments is presented. (F) Effects of carbachol and PDBu on BSM contraction in permeabilized WT and c-Rel KO tissue. Alpha-toxin-permeabilized BSM strips were contracted with low Ca^{2+} (pCa 7.5) alone, with low Ca^{2+} (pCa 7.5) plus carbachol plus GTP, or with low Ca^{2+} (pCa 7.5) plus PDBu. Contractions were normalized to the maximal response elicited by pCa 4.5. Data are presented as the means ± SD of five experiments. $n = 5$; **, $P < 0.05$ compared with low Ca^{2+} alone; pCa 7.5.

Kim et al. reported that Sp1 and Sp3 regulate CPI-17 gene expression through a multiple-kinase pathway via GC boxes in the promoter and that a proximal GATA motif adjacent to the GC boxes is also required for CPI-17 gene expression in aortic smooth muscle (19). This is in agreement with our findings that GATA motifs activate CPI-17 promoter activity in murine and human BSM cells.

Activation of NF-κB has been implicated in many physiological and pathological processes, including inflammation, immune cell maturation, cell survival, and cardiac muscle hypertrophy (47–50). The proinflammatory cytokines TNF-α and IL-1β downregulate CPI-17 expression and inhibit intestinal and colonic smooth muscle contraction (18, 51). In contrast, CPI-17 transcription in aortic smooth muscle is increased by TGF-β, IL-1β, and TNF-α (19). Earlier studies have demonstrated that NF-κB regulates IL-1β transcription (52); however, a direct relationship between NF-κB and CPI-17 has not yet been demonstrated. In this study, we show for the first time that NF-κB induces CPI-17 transcription in BSM. Since IL-1β upregulates CPI-17 expression in aortic smooth muscle (19), it is possible that this cytokine increases CPI-17 expression in BSM through NF-κB p50 and c-Rel. However, Kim et al. demonstrated that silencing of NF-κB p65 (RelA) expression did not change the level of CPI-17 expression in aortic smooth muscle (19), whereas our study unequivocally demonstrated that NF-κB p50 and c-Rel positively regulate CPI-17 gene expression in murine and human BSM. This discrepancy may be due to either tissue-specific regulation of CPI-17 by NF-κB or the involvement of different isoforms of NF-κB in the regulation of CPI-17 gene expression in aortic and bladder smooth muscle, as suggested by our failure to detect NF-κB p65 in the purified fractions from CPI-17 promoter DNA affinity column chromatography of murine BSM nuclear extract. NF-κB exists in unstimulated cells as an inactive heterotrimeric complex comprised of p50 and p65 or p50 and c-Rel subunits bound to their cytosolic inhibitor protein, IκBα (47, 53). The canonical NF-κB signaling pathway involves the phosphorylation-dependent degradation of IκB by activated IκB kinase (IKK) complex, resulting in nuclear translocation of NF-κB dimers and transcriptional regulation of specific target genes (47, 53). Despite this well-established and accepted paradigm for signal-induced

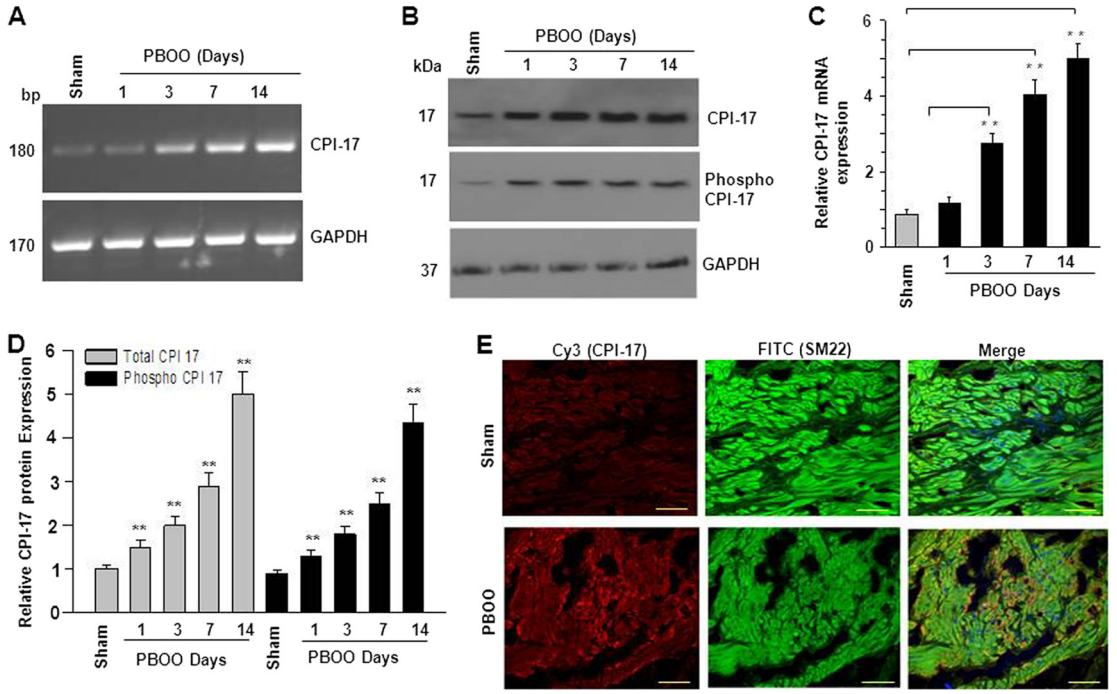

FIG 10 Overexpression of CPI-17 in murine model of PBOO. (A and B) RT-PCR (A) and immunoblot (B) analysis of CPI-17 mRNA and protein expression in sham-operated and PBOO mouse BSM tissues. GAPDH served as a control. (C and D) Quantification of RT-PCR (A) and immunoblot (B) data presented as means ± SD ($n = 10$ each for sham-operated and PBOO mouse BSM). **, $P < 0.01$ compared with the results for sham-operated control mice. (E) Murine bladder sections prepared from sham-operated and PBOO mice were stained with anti-CPI-17 (Cy3, red) and anti-SM22 (FITC, green) antibodies. Negative-control sections were prepared using antibody preabsorbed with the antigen used to raise the antibody (data not shown). Scale bars = 20 μm.

NF-κB activation, there is growing evidence that NF-κB is present in the nucleus in unstimulated cells and constitutively silences gene transcription by competing with other transcription factors (54). In accordance with earlier observations, we observed the presence of nuclear NF-κB in murine and human BSM. Increased expression and nuclear localization of NF-κB were positively correlated with the transcriptional upregulation of CPI-17 in obstructed BSM.

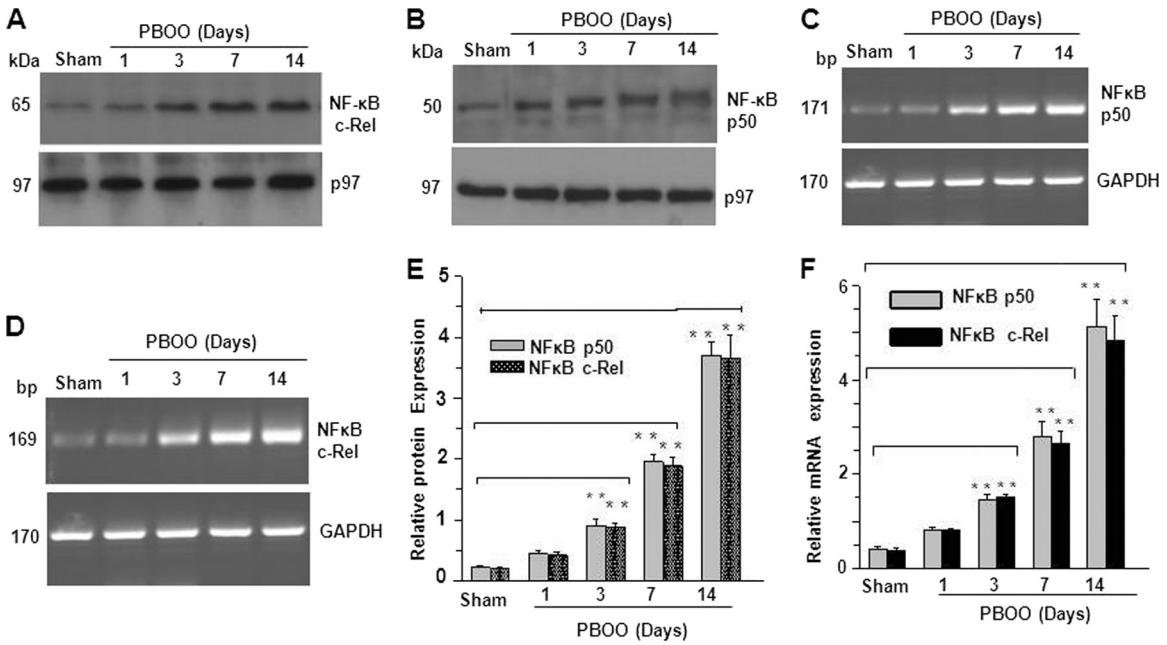

FIG 11 Overexpression of NF-κB p50 and c-Rel in murine model of PBOO. Nuclear protein (A and B) and RNA (C and D) were prepared from sham-operated and PBOO mouse BSM tissues and analyzed for NF-κB p50, c-Rel, GAPDH, and p97 expression. GAPDH and p97 served as loading controls. (E and F) Data are presented as means ± SD ($n = 10$ each for sham-operated and PBOO mice). **, $P < 0.01$ compared with sham-operated control mice.

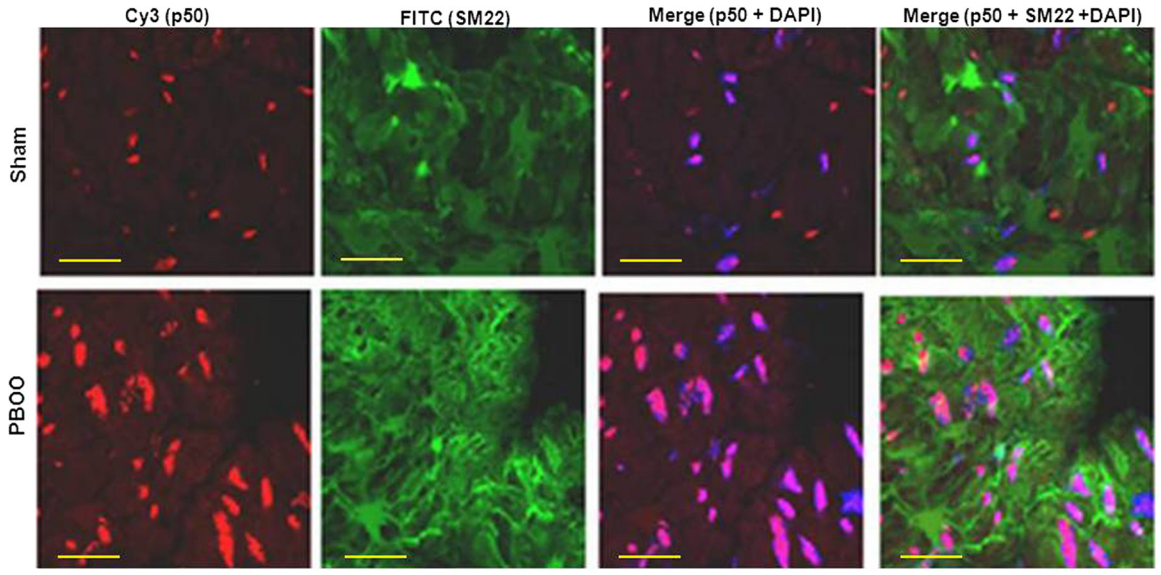

FIG 12 *In situ* localization of NF-κB p50 in murine model of PBOO. Bladder sections prepared from sham-operated and PBOO mice were stained with anti-NF-κB p50 (Cy3, red) and anti-SM22 (FITC, green). Scale bars = 15 μm.

The vertebrate GATA motif WGATAR (where W is A or T and R is A or G) is a DNA sequence element that was initially defined in the promoters of erythroid cell globin genes (55, 56), and similar GATA motifs have since been described in the promoters of various genes involved in the proliferation and differentiation of cardiac and smooth muscle cells (57–63). Members of the GATA family of transcription factors, which bind the consensus DNA-binding motif 5′-GATA-3′ in target gene promoters and enhancers (56), possess a DNA-binding domain consisting of two distinct zinc finger domains with an adjacent highly conserved basic region (64, 65). Six members of the GATA family of zinc finger transcription factors have been identified: GATA-1, -2, -3, -4, -5, and -6 (60). GATA-6 is expressed in heart, muscle, and smooth muscle tissue in the respiratory tract, arteries, bronchi, and urogenital tract, including the urinary bladder (66). GATA-6 directly controls the expression of various contractile and signaling proteins in cardiac and smooth muscles (67–69), and loss of the GATA-6 gene leads to defects in embryonic development and lethality (66). Activation of GATA-4 and GATA-6 is strongly associated with physiological and pathological cardiac and smooth muscle hypertrophy (20, 70–72). In this study, we demonstrate for the first time that GATA-6 activates CPI-17 promoter activity by

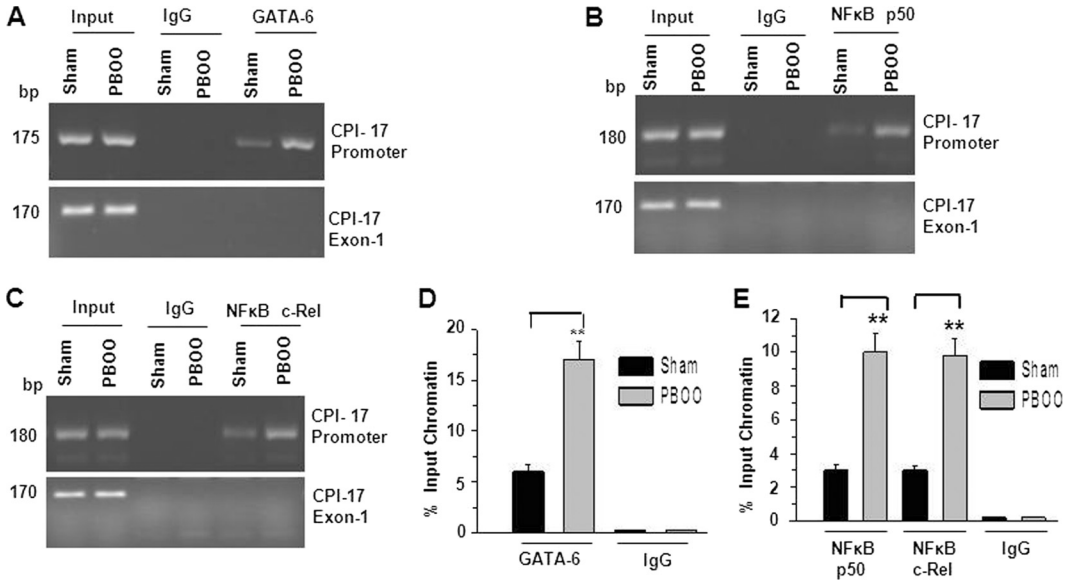

FIG 13 PBOO increased NF-κB and GATA-6 DNA binding activity. (A to C) Chromatin samples prepared from sham-operated and PBOO mouse BSM were immunoprecipitated with anti-GATA-6, NF-κB p50, and c-Rel antibodies or preimmune rabbit serum. Precipitated fragments were PCR amplified using primers specific for GATA and κB motifs on the mouse CPI-17 promoter or primers specific for CPI-17 exon-1 as a negative control. (D and E) Quantification of band intensities from agarose gels is presented as percentages of input chromatin (average of six sham-operated and six PBOO mouse samples). Data are presented as means ± SD. **, $P < 0.01$ compared with the results for sham-operated control mice.

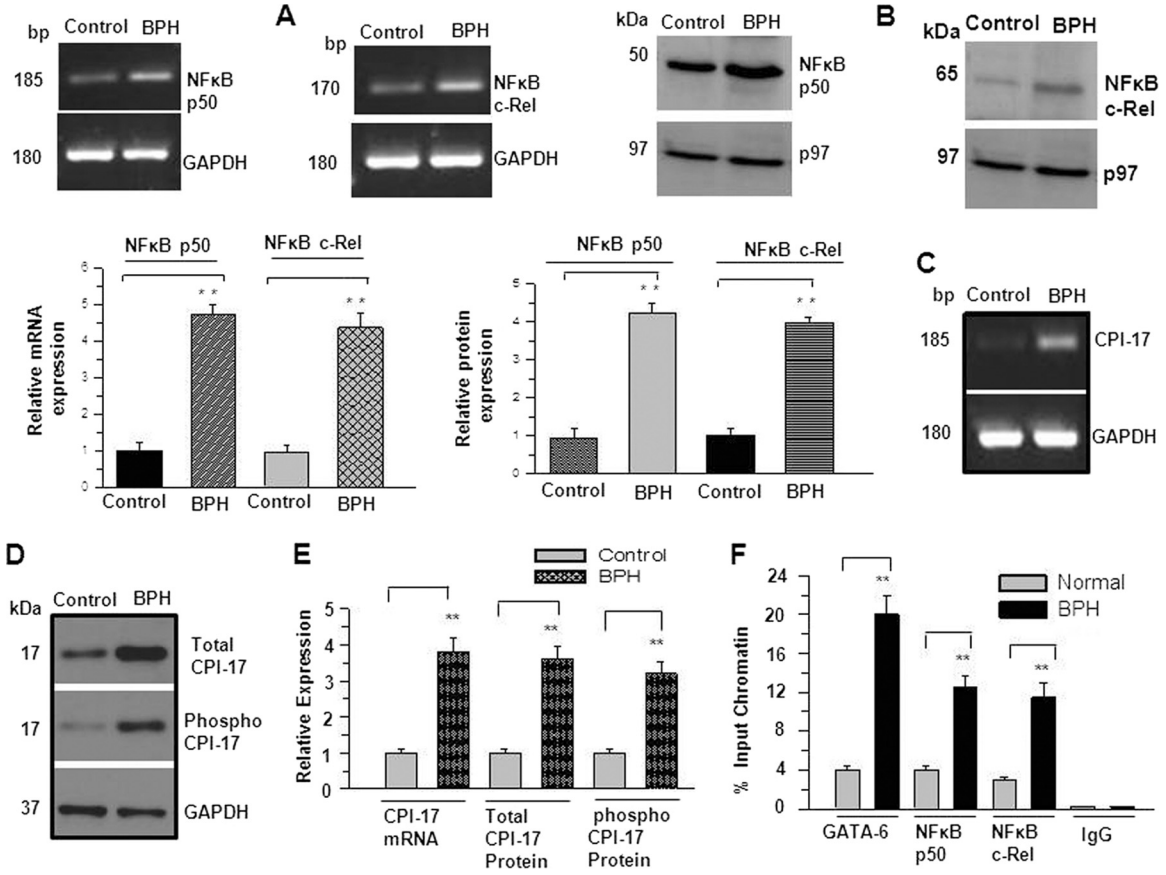

FIG 14 Overexpression of NF-κB and GATA-6 in BPH-induced bladder outlet obstruction correlates with CPI-17 gene expression. (A to E) RNA and protein samples prepared from BSM of control and BPH patients were subjected to RT-PCR and immunoblot analysis for NF-κB p50, c-Rel, CPI-17, and phospho-CPI-17. GAPDH and p97 were used as controls. Data are presented as means ± SD. **, $P < 0.01$ compared with the results for control human BSM. (F) Chromatin samples from BSM of control and BPH patients were immunoprecipitated with antibodies specific for GATA-6, NF-κB p50, and c-Rel or preimmune rabbit IgG. Precipitated fragments were PCR amplified using primers specific for GATA and κB motifs in the human CPI-17 promoter. Rabbit IgG was used as a negative control. Quantification of band intensities from agarose gels is presented as percentage of input chromatin. Data are presented as means ± SD. **, $P < 0.01$ compared with the results for control human BSM.

binding to the GATA sequence in the promoter and increases CPI-17 mRNA and protein expression. The additive effect of GATA-6 and NF-κB on CPI-17 transcriptional activation probably contributes to the significant upregulation of CPI-17 gene expression that was observed in murine and human pathological BSM hypertrophy. The activating effects of these transcription factors on the CPI-17 promoter were strong alone; however, their additive effect was much stronger, perhaps due to protein-protein interactions between GATA-6, NF-κB p50, and c-Rel.

To completely empty the bladder, the BSM must generate and maintain a maximum amount of force. The maximum force generation in the early phase of contraction and MLC_{20} phosphorylation is governed by activation of Ca^{2+}/calmodulin-dependent MLCK, while the PKC and RhoA pathway, mediated through CPI-17 and MYPT1, respectively, in response to agonist stimulation, plays a major role in force generation and maintenance by inhibiting MLC phosphatase activity (2). Low MLCP activity results in maintenance of the phosphorylated state of myosin, allowing the muscle to develop tone at low Ca^{2+} concentrations (2). Carbachol stimulation activates the $G_{q/11}$-phospholipase Cβ-PKC and the $G_{12/13}$-RhoA-ROCK pathways through binding to muscarinic receptors in bladder smooth muscle (73). We found that BSM from c-Rel KO mice exhibits lower force maintenance than that from WT mice during sustained contraction in response to carbachol, despite the increase in CPI-17 phosphorylation. However, c-Rel mice have a significantly reduced overall amount of phosphorylated CPI-17 compared to that of WT mice due to the decreased amount of total CPI-17 protein. These results suggest that, in addition to Rho kinase, CPI-17 is required for force maintenance during sustained contraction.

Experiments on c-Rel KO mouse bladders suggest that both receptor-independent and G protein receptor-dependent BSM requires CPI-17 for force maintenance during sustained contraction. In addition, the significant loss of CPI-17 in c-Rel KO mouse bladders suppressed PDBu-stimulated BSM contraction. Together, our results suggest that the transcription factor NF-κB is required for PDBu-mediated BSM contraction and is involved in force maintenance during sustained contraction in receptor-dependent and -independent BSM contraction.

Overexpression of CPI-17 in vascular smooth muscle from type 2 diabetic db/db mice is correlated with hypercontractility of tissues (15). Earlier studies have reported that there is a high level of basal MLC_{20} phosphorylation and increased spontane-

ous contraction in BSM of PBOO (74) and diabetic (14) rabbits. We hypothesize that overexpression of CPI-17 is a contributing factor in the increased basal MLC_{20} phosphorylation in murine PBOO BSM and that this may contribute to bladder overactivity in BPH patients. In addition, increased expression of CPI-17 and ROCKβ may be responsible in part for the high degree of force maintenance and slow relaxation of rabbit BSM that was observed in earlier studies of outlet obstruction (43) and diabetes (14).

In summary, GATA-6, NF-κB p50, and c-Rel act as transcriptional activators of CPI-17 transcription and NF-κB regulates PKC-mediated contraction in BSM. The expression of these transcription factors in BSM from obstructed bladders and cultured cells was positively correlated with the expression of total and phospho-CPI-17. Taken together, the results of this study provide the molecular mechanism of CPI-17 overexpression during pathological smooth muscle hypertrophy and implicate these transcriptional factors as potential therapeutic targets for the treatment of bladder overactivity in BPH patients. Currently available drugs to control overactive bladder have drawbacks with respect to their efficacy and side effects, and these limitations may be overcome by targeting the upregulation of GATA-6- and NF-κB-mediated CPI-17 transcription in men with BPH-induced bladder dysfunction. In addition, our findings may serve as a basis for future studies aimed at understanding GATA-6- and NF-κB-regulated physiological and pathological signaling in smooth muscle differentiation and contraction.

ACKNOWLEDGMENTS

We thank Christopher Hunter and Hsiou-Chi Lieu for providing the bladder tissue from NF-κB p50 mice and the NF-κB c-Rel breeding colony. We thank Ranjita Chackaraborty for help in immunofluorescence analysis. We also thank Jocelyn McCabe for help in preparing the manuscript.

This study was supported by O'Brien Urology Research Center grant P50 DK052620 from NIDDK.

REFERENCES

1. **Adelstein RS, Eisenberg E.** 1980. Regulation and kinetics of the actin-myosin-ATP interaction. Annu. Rev. Biochem. **49**:921–956.
2. **Somlyo AP, Somlyo AV.** 2003. Ca2+ sensitivity of smooth muscle and nonmuscle myosin II: modulated by G proteins, kinases, and myosin phosphatase. Physiol. Rev. **83**:1325–1358.
3. **Somlyo AP, Somlyo AV.** 2000. Signal transduction by G-proteins, rho-kinase and protein phosphatase to smooth muscle and non-muscle myosin II. J. Physiol. **522**(Pt 2):177–185.
4. **Mizuno Y, Isotani E, Huang J, Ding H, Stull JT, Kamm KE.** 2008. Myosin light chain kinase activation and calcium sensitization in smooth muscle in vivo. Am. J. Physiol. Cell Physiol. **295**:C358–C364.
5. **Wang T, Kendig DM, Smolock EM, Moreland RS.** 2009. Carbachol-induced rabbit bladder smooth muscle contraction: roles of protein kinase C and Rho kinase. Am. J. Physiol. Renal Physiol. **297**:F1534–F1542.
6. **Woodsome TP, Eto M, Everett A, Brautigan DL, Kitazawa T.** 2001. Expression of CPI-17 and myosin phosphatase correlates with Ca(2+) sensitivity of protein kinase C-induced contraction in rabbit smooth muscle. J. Physiol. **535**:553–564.
7. **Eto M, Bock R, Brautigan DL, Linden DJ.** 2002. Cerebellar long-term synaptic depression requires PKC-mediated activation of CPI-17, a myosin/moesin phosphatase inhibitor. Neuron **36**:1145–1158.
8. **Eto M, Ohmori T, Suzuki M, Furuya K, Morita F.** 1995. A novel protein phosphatase-1 inhibitory protein potentiated by protein kinase C. Isolation from porcine aorta media and characterization. J. Biochem. **118**:1104–1107.
9. **Eto M, Senba S, Morita F, Yazawa M.** 1997. Molecular cloning of a novel phosphorylation-dependent inhibitory protein of protein phosphatase-1 (CPI17) in smooth muscle: its specific localization in smooth muscle. FEBS Lett. **410**:356–360.
10. **Ohama T, Hori M, Sato K, Ozaki H, Karaki H.** 2003. Chronic treatment with interleukin-1beta attenuates contractions by decreasing the activities of CPI-17 and MYPT-1 in intestinal smooth muscle. J. Biol. Chem. **278**:48794–48804.
11. **Sakai H, Chiba Y, Hirano T, Misawa M.** 2005. Possible involvement of CPI-17 in augmented bronchial smooth muscle contraction in antigen-induced airway hyper-responsive rats. Mol. Pharmacol. **68**:145–151.
12. **Dakshinamurti S, Mellow L, Stephens NL.** 2005. Regulation of pulmonary arterial myosin phosphatase activity in neonatal circulatory transition and in hypoxic pulmonary hypertension: a role for CPI-17. Pediatr. Pulmonol. **40**:398–407.
13. **Eto M, Kitazawa T, Yazawa M, Mukai H, Ono Y, Brautigan DL.** 2001. Histamine-induced vasoconstriction involves phosphorylation of a specific inhibitor protein for myosin phosphatase by protein kinase C alpha and delta isoforms. J. Biol. Chem. **276**:29072–29078.
14. **Chang S, Hypolite JA, DiSanto ME, Changolkar A, Wein AJ, Chacko S.** 2006. Increased basal phosphorylation of detrusor smooth muscle myosin in alloxan-induced diabetic rabbit is mediated by upregulation of Rho-kinase beta and CPI-17. Am. J. Physiol. Renal Physiol. **290**:F650–F656.
15. **Xie Z, Su W, Guo Z, Pang H, Post SR, Gong MC.** 2006. Upregulation of CPI-17 phosphorylation in diabetic vasculature and high glucose cultured vascular smooth muscle cells. Cardiovasc. Res. **69**:491–501.
16. **Chang S, Hypolite JA, Mohanan S, Zderic SA, Wein AJ, Chacko S.** 2009. Alteration of the PKC-mediated signaling pathway for smooth muscle contraction in obstruction-induced hypertrophy of the urinary bladder. Lab. Invest. **89**:823–832.
17. **Jin H, Sperka T, Herrlich P, Morrison H.** 2006. Tumorigenic transformation by CPI-17 through inhibition of a merlin phosphatase. Nature **442**:576–579.
18. **Hu W, Mahavadi S, Li F, Murthy KS.** 2007. Upregulation of RGS4 and downregulation of CPI-17 mediate inhibition of colonic muscle contraction by interleukin-1beta. Am. J. Physiol. Cell Physiol. **293**:C1991–C2000.
19. **Kim JI, Urban M, Young GD, Eto M.** 2012. Reciprocal regulation controlling the expression of CPI-17, a specific inhibitor protein for the myosin light chain phosphatase in vascular smooth muscle cells. Am. J. Physiol. Cell Physiol. **303**:C58–C68.
20. **Boopathi E, Gomes CM, Goldfarb R, John M, Srinivasan VG, Alanzi J, Malkowicz SB, Kathuria H, Zderic SA, Wein AJ, Chacko S.** 2011. Transcriptional repression of caveolin-1 (CAV1) gene expression by GATA-6 in bladder smooth muscle hypertrophy in mice and human beings. Am. J. Pathol. **178**:2236–2251.
21. **Thompson JD, Higgins DG, Gibson TJ.** 1994. CLUSTAL W: improving the sensitivity of progressive multiple sequence alignment through sequence weighting, position-specific gap penalties and weight matrix choice. Nucleic Acids Res. **22**:4673–4680.
22. **Austin JC, Chacko SK, DiSanto M, Canning DA, Zderic SA.** 2004. A male murine model of partial bladder outlet obstruction reveals changes in detrusor morphology, contractility and myosin isoform expression. J. Urol. **172**:1524–1528.
23. **Masternak K, Muhlethaler-Mottet A, Villard J, Zufferey M, Steimle V, Reith W.** 2000. CIITA is a transcriptional coactivator that is recruited to MHC class II promoters by multiple synergistic interactions with an enhanceosome complex. Genes Dev. **14**:1156–1166.
24. **Kadonaga JT, Tjian R.** 1986. Affinity purification of sequence-specific DNA binding proteins. Proc. Natl. Acad. Sci. U. S. A. **83**:5889–5893.
25. **Dignam JD, Lebovitz RM, Roeder RG.** 1983. Accurate transcription initiation by RNA polymerase II in a soluble extract from isolated mammalian nuclei. Nucleic Acids Res. **11**:1475–1489.
26. **Singh H, Sen R, Baltimore D, Sharp PA.** 1986. A nuclear factor that binds to a conserved sequence motif in transcriptional control elements of immunoglobulin genes. Nature **319**:154–158.
27. **Boopathi E, Lenka N, Prabu SK, Fang JK, Wilkinson F, Atchison M, Giallongo A, Avadhani NG.** 2004. Regulation of murine cytochrome c oxidase Vb gene expression during myogenesis: YY-1 and heterogeneous nuclear ribonucleoprotein D-like protein (JKTBP1) reciprocally regulate transcription activity by physical interaction with the BERF-1/ZBP-89 factor. J. Biol. Chem. **279**:35242–35254.

28. **O'Neill LP, Turner BM.** 1995. Histone H4 acetylation distinguishes coding regions of the human genome from heterochromatin in a differentiation-dependent but transcription-independent manner. EMBO J. **14**: 3946–3957.
29. **Polyak E, Boopathi E, Mohanan S, Deng M, Zderic SA, Wein AJ, Chacko S.** 2009. Alterations in caveolin expression and ultrastructure after bladder smooth muscle hypertrophy. J. Urol. **182**:2497–2503.
30. **Schreiber E, Matthias P, Muller MM, Schaffner W.** 1989. Rapid detection of octamer binding proteins with 'mini-extracts,' prepared from a small number of cells. Nucleic Acids Res. **17**:6419.
31. **Anderson DJ, Blobel G.** 1983. Immunoprecipitation of proteins from cell-free translations. Methods Enzymol. **96**:111–120.
32. **Zhang EY, Stein R, Chang S, Zheng Y, Zderic SA, Wein AJ, Chacko S.** 2004. Smooth muscle hypertrophy following partial bladder outlet obstruction is associated with overexpression of non-muscle caldesmon. Am. J. Pathol. **164**:601–612.
33. **Hypolite JA, Chang S, LaBelle E, Babu GJ, Periasamy M, Wein AJ, Chacko S.** 2009. Deletion of SM-B, the high ATPase isoform of myosin, upregulates the PKC-mediated signal transduction pathway in murine urinary bladder smooth muscle. Am. J. Physiol. Renal Physiol. **296**:F658–F665.
34. **Hypolite JA, DiSanto ME, Zheng Y, Chang S, Wein AJ, Chacko S.** 2001. Regional variation in myosin isoforms and phosphorylation at the resting tone in urinary bladder smooth muscle. Am. J. Physiol. Cell Physiol. **280**: C254–C264.
35. **Stanton MC, Delaney D, Zderic SA, Moreland RS.** 2004. Partial bladder outlet obstruction abolishes the receptor- and G protein-dependent increase in calcium sensitivity in rabbit bladder smooth muscle. Am. J. Physiol. Renal Physiol. **287**:F682–F689.
36. **Fabiato A.** 1988. Computer programs for calculating total from specified free or free from specified total ionic concentrations in aqueous solutions containing multiple metals and ligands. Methods Enzymol. **157**:378–417.
37. **Moreland RS, Murphy RA.** 1986. Determinants of Ca2+-dependent stress maintenance in skinned swine carotid media. Am. J. Physiol. **251**:C892–C903.
38. **Cartharius K, Frech K, Grote K, Klocke B, Haltmeier M, Klingenhoff A, Frisch M, Bayerlein M, Werner T.** 2005. MatInspector and beyond: promoter analysis based on transcription factor binding sites. Bioinformatics **21**:2933–2942.
39. **Wang T, Kendig DM, Trappanese DM, Smolock EM, Moreland RS.** 2012. Phorbol 12,13-dibutyrate-induced, protein kinase C-mediated contraction of rabbit bladder smooth muscle. Front. Pharmacol. **2**:83. doi:10.3389/fphar.2011.00083.
40. **Fulginiti J, III, Singer HA, Moreland RS.** 1993. Phorbol ester-induced contractions of swine carotid artery are supported by slowly cycling cross-bridges which are not dependent on calcium or myosin light chain phosphorylation. J. Vasc. Res. **30**:315–322.
41. **Abrams P, Donovan JL, de la Rosette JJ, Schafer W.** 1997. International Continence Society "Benign Prostatic Hyperplasia" study: background, aims, and methodology. Neurourol. Urodyn. **16**:79–91.
42. **Levin RM, Haugaard N, O'Connor L, Buttyan R, Das A, Dixon JS, Gosling JA.** 2000. Obstructive response of human bladder to BPH vs. rabbit bladder response to partial outlet obstruction: a direct comparison. Neurourol. Urodyn. **19**:609–629.
43. **Bing W, Chang S, Hypolite JA, DiSanto ME, Zderic SA, Rolf L, Wein AJ, Chacko S.** 2003. Obstruction-induced changes in urinary bladder smooth muscle contractility: a role for Rho kinase. Am. J. Physiol. Renal Physiol. **285**:F990–F997.
44. **Chang S, Gomes CM, Hypolite JA, Marx J, Alanzi J, Zderic SA, Malkowicz B, Wein AJ, Chacko S.** 2010. Detrusor overactivity is associated with downregulation of large-conductance calcium- and voltage-activated potassium channel protein. Am. J. Physiol. Renal Physiol. **298**: F1416–F1423.
45. **Clement MR, Delaney DP, Austin JC, Sliwoski J, Hii GC, Canning DA, DiSanto ME, Chacko SK, Zderic SA.** 2006. Activation of the calcineurin pathway is associated with detrusor decompensation: a potential therapeutic target. J. Urol. **176**:1225–1229.
46. **DiSanto ME, Stein R, Chang S, Hypolite JA, Zheng Y, Zderic S, Wein AJ, Chacko S.** 2003. Alteration in expression of myosin isoforms in detrusor smooth muscle following bladder outlet obstruction. Am. J. Physiol. Cell Physiol. **285**:C1397–C1410.
47. **Baeuerle PA, Baltimore D.** 1996. NF-kappa B: ten years after. Cell **87**:13–20.
48. **Gaspar-Pereira S, Fullard N, Townsend PA, Banks PS, Ellis EL, Fox C, Maxwell AG, Murphy LB, Kirk A, Bauer R, Caamano JH, Figg N, Foo RS, Mann J, Mann DA, Oakley F.** 2012. The NF-kappaB subunit c-Rel stimulates cardiac hypertrophy and fibrosis. Am. J. Pathol. **180**:929–939.
49. **Karin M, Lin A.** 2002. NF-kappaB at the crossroads of life and death. Nat. Immunol. **3**:221–227.
50. **Shaw J, Yurkova N, Zhang T, Gang H, Aguilar F, Weidman D, Scramstad C, Weisman H, Kirshenbaum LA.** 2008. Antagonism of E2F-1 regulated Bnip3 transcription by NF-kappaB is essential for basal cell survival. Proc. Natl. Acad. Sci. U. S. A. **105**:20734–20739.
51. **Ohama T, Hori M, Momotani E, Iwakura Y, Guo F, Kishi H, Kobayashi S, Ozaki H.** 2007. Intestinal inflammation downregulates smooth muscle CPI-17 through induction of TNF-alpha and causes motility disorders. Am. J. Physiol. Gastrointest. Liver Physiol. **292**: G1429–G1438.
52. **Cogswell JP, Godlevski MM, Wisely GB, Clay WC, Leesnitzer LM, Ways JP, Gray JG.** 1994. NF-kappa B regulates IL-1 beta transcription through a consensus NF-kappa B binding site and a nonconsensus CRE-like site. J. Immunol. **153**:712–723.
53. **Karin M.** 1999. The beginning of the end: IkappaB kinase (IKK) and NF-kappaB activation. J. Biol. Chem. **274**:27339–27342.
54. **Purcell NH, Tang G, Yu C, Mercurio F, DiDonato JA, Lin A.** 2001. Activation of NF-kappa B is required for hypertrophic growth of primary rat neonatal ventricular cardiomyocytes. Proc. Natl. Acad. Sci. U. S. A. **98**:6668–6673.
55. **Evans T, Reitman M, Felsenfeld G.** 1988. An erythrocyte-specific DNA-binding factor recognizes a regulatory sequence common to all chicken globin genes. Proc. Natl. Acad. Sci. U. S. A. **85**:5976–5980.
56. **Orkin SH.** 1992. GATA-binding transcription factors in hematopoietic cells. Blood **80**:575–581.
57. **Burch JB.** 2005. Regulation of GATA gene expression during vertebrate development. Semin. Cell Dev. Biol. **16**:71–81.
58. **Kanematsu A, Ramachandran A, Adam RM.** 2007. GATA-6 mediates human bladder smooth muscle differentiation: involvement of a novel enhancer element in regulating alpha-smooth muscle actin gene expression. Am. J. Physiol. Cell Physiol. **293**:C1093–C1102.
59. **Lien CL, Wu C, Mercer B, Webb R, Richardson JA, Olson EN.** 1999. Control of early cardiac-specific transcription of Nkx2-5 by a GATA-dependent enhancer. Development **126**:75–84.
60. **Molkentin JD.** 2000. The zinc finger-containing transcription factors GATA-4, -5, and -6. Ubiquitously expressed regulators of tissue-specific gene expression. J. Biol. Chem. **275**:38949–38952.
61. **Molkentin JD, Tymitz KM, Richardson JA, Olson EN.** 2000. Abnormalities of the genitourinary tract in female mice lacking GATA5. Mol. Cell. Biol. **20**:5256–5260.
62. **Oh J, Wang Z, Wang DZ, Lien CL, Xing W, Olson EN.** 2004. Target gene-specific modulation of myocardin activity by GATA transcription factors. Mol. Cell. Biol. **24**:8519–8528.
63. **Xin M, Davis CA, Molkentin JD, Lien CL, Duncan SA, Richardson JA, Olson EN.** 2006. A threshold of GATA4 and GATA6 expression is required for cardiovascular development. Proc. Natl. Acad. Sci. U. S. A. **103**:11189–11194.
64. **Ko LJ, Engel JD.** 1993. DNA-binding specificities of the GATA transcription factor family. Mol. Cell. Biol. **13**:4011–4022.
65. **Sakai Y, Nakagawa R, Sato R, Maeda M.** 1998. Selection of DNA binding sites for human transcriptional regulator GATA-6. Biochem. Biophys. Res. Commun. **250**:682–688.
66. **Morrisey EE, Ip HS, Lu MM, Parmacek MS.** 1996. GATA-6: a zinc finger transcription factor that is expressed in multiple cell lineages derived from lateral mesoderm. Dev. Biol. **177**:309–322.
67. **Chang DF, Belaguli NS, Iyer D, Roberts WB, Wu SP, Dong XR, Marx JG, Moore MS, Beckerle MC, Majesky MW, Schwartz RJ.** 2003. Cysteine-rich LIM-only proteins CRP1 and CRP2 are potent smooth muscle differentiation cofactors. Dev. Cell **4**:107–118.
68. **Shirvani S, Xiang F, Koibuchi N, Chin MT.** 2006. CHF1/Hey2 suppresses SM-MHC promoter activity through an interaction with GATA-6. Biochem. Biophys. Res. Commun. **339**:151–156.
69. **Yin F, Herring BP.** 2005. GATA-6 can act as a positive or negative regulator of smooth muscle-specific gene expression. J. Biol. Chem. **280**:4745–4752.
70. **Molkentin JD, Lu JR, Antos CL, Markham B, Richardson J, Robbins J, Grant SR, Olson EN.** 1998. A calcineurin-dependent transcriptional pathway for cardiac hypertrophy. Cell **93**:215–228.

71. **Molkentin JD, Olson EN.** 1997. GATA4: a novel transcriptional regulator of cardiac hypertrophy? Circulation **96**:3833–3835.
72. **van Berlo JH, Elrod JW, van den Hoogenhof MM, York AJ, Aronow BJ, Duncan SA, Molkentin JD.** 2010. The transcription factor GATA-6 regulates pathological cardiac hypertrophy. Circ. Res. **107**: 1032–1040.
73. **Peters SL, Schmidt M, Michel MC.** 2006. Rho kinase: a target for treating urinary bladder dysfunction? Trends Pharmacol. Sci. **27**:492–497.
74. **Su X, Stein R, Stanton MC, Zderic S, Moreland RS.** 2003. Effect of partial outlet obstruction on rabbit urinary bladder smooth muscle function. Am. J. Physiol. Renal Physiol. **284**:F644–F652.